ISTANBUL TECHNICAL UNIVERSITY ★ GRADUATE SCHOOL OF SCIENCE ENGINEERING AND TECHNOLOGY

EVALUATION OF REYNOLDS STRESSES IN SEDIMENT FLUSHING IN AN OPEN CHANNEL FLOW

M.Sc. THESIS

Erdem ÇELENK

Department of Civil Engineering

Hydraulics and Water Resources Engineering Program

DECEMBER 2019

ISTANBUL TECHNICAL UNIVERSITY ★ GRADUATE SCHOOL OF SCIENCE ENGINEERING AND TECHNOLOGY

EVALUATION OF REYNOLDS STRESSES IN SEDIMENT FLUSHING IN AN OPEN CHANNEL FLOW

M.Sc. THESIS

Erdem ÇELENK
(501161517)

Department of Civil Engineering

Hydraulics and Water Resources Engineering Program

Thesis Advisor: Prof. Dr. Şevket ÇOKGÖR

DECEMBER 2019

ISTANBUL TEKNİK ÜNİVERSİTESİ ★ FEN BİLİMLERİ ENSTİTÜSÜ

AÇIK KANALDAKİ REYNOLDS GERİLMELERİNİN SEDİMENT YIKAMA İŞLEMİ SIRASINDA DEĞERLENDİRİLMESİ

YÜKSEK LİSANS TEZİ

Erdem ÇELENK
(501161517)

İnşaat Mühendisliği Anabilim Dalı

Hidrolik ve Su Kaynakları Mühendisliği Programı

Tez Danışmanı: Prof. Dr. Şevket ÇOKGÖR

ARALIK 2019

Erdem Çelenk, a M.Sc. student of ITU Graduate School of Science Engineering and Technology student ID 501161517, successfully defended the thesis entitled "EVALUATION OF REYNOLDS STRESSES IN SEDIMENT FLUSHING IN AN OPEN CHANNEL FLOW",
which he prepared after fulfilling the requirements specified in the associated legislations, before the jury whose signatures are below.

Thesis Advisor:	**Prof. Dr. Şevket ÇOKGÖR** Istanbul Technical University	.....
Jury Members:	**Doç. Dr. Oral YAĞCI** Istanbul Technical University	.....
	Doç. Dr. Berna AYAT AYDOĞAN Yıldız Technical University	.....

Date of Submission : 15 November 2019
Date of Defense : 27 December 2019

To my family,

FOREWORD

This thesis is written in the dates between March 2019 and November 2019 during my graduate study at Istanbul Technical University. I have received lots of help from my advisor Prof. Dr. Şevket Çokgör anytime I needed. Not only his precious guidance during my graduate study but also his understanding to my both technical and personal issues and questions have certainly played a crucial role during this compelling period. I hereby present my thanks to him for his marvelous support. I also should thank to Assoc. Prof. Dr. Veysel Şadan Özgür Kırca for his special attention and guidance when I was studying on the projects of Advanced Fluid Mechanics and Turbulence courses, which have truly helped me to comprehend Hydrodynamics. Moreover, I am very grateful to my family, my mother Ayşe Çelenk, my father Ünal Çelenk and my twin brother Onur Çelenk M.D, for their emotional support throughout difficult and challenging times. I also present my special thanks to my colleagues at work and my manager Nergis Yavaş, the design manager of Marmaray CR3 Project as she allowed me a day's absence anytime I asked for.

Finally, I thank to my girlfriend Pelin Emecan who is a very receptive mathematician, for her love and unflagging support. I must admit that this thesis could never be completed without her.

November 2019

Erdem ÇELENK
(Civil Engineer)

TABLE OF CONTENTS

ABBREVIATIONS

RCC : Roller Compacted Concrete

ADV : Acoustic Doppler Velocimeter

ITU : Istanbul Technical University

HPP : Hydropower Plant

ICOLD : International Commission on Large Dams

PVC :Polyvinyl Chloride

IRTCES :The International Research and Training Center on Erosion and Sedimentation

USSR : Union of Soviet Socialist Republics

LIST OF TABLES

Page

LIST OF FIGURES

EVALUATION OF REYNOLDS STRESSES IN SEDIMENT FLUSHING IN AN OPEN CHANNEL FLOW

SUMMARY

Determination of reservoir capacity has been always a significant part of the dam design process. A reservoir's capacity is calculated by using some certain methods such as Mass Curve Analysis, Sequent Peak Analysis and Operation Study. A prospective dead storage volume is also calculated by estimating the annual sediment yield utilizing some empirical formulas and then by predicting of trap efficiency, which is defined as the retained inflowing sediment of the reservoir in percentage. Trap efficiency may be also identified as a function of the ratio of the reservoir capacity to total inflow. Because of the fact that sediment accumulation is difficult to predict since the accumulation in general can vary from low amounts to large ones depending on the magnitude of the inflow to the reservoir, the calculated dead storage values might not reflect the real amounts faced in future. That sort of mistaken predictions brings about losing large amount of money as the dam cannot be run in the estimated capacity due to the unexpected sediment quantity. To regain the capacity of reservoir, some techniques are applied such as sluicing, syphoning and dredging and flushing which is the most common technique used across the world. Moreover, a few irregularities in operation of the whole river basin cause unexpected amounts of sediment accumulation. For instance, disrupting the basin planning by commencing a dam's construction before another, whose construction should have been primarily started is one of these irregularities. In our case, the problem faced is out of a similar disruption.

Laleli, İspir and Güllübağ dams were planned to be built on the main branch of the Çoruh river which is one of the fastest rivers in the world by discharge volume. Even though its discharge volume is variable year by year, it usually has an average discharge volume over 200 m^3/s. All these three dams play a key role in the regulation of both water potential and sediment accumulation in Çoruh basin. In this context, Laleli, İspir and then Güllübağ dams respectively should have been turned into investment. Yet, due to some financial reasons, it was decided to commence Güllübağ Dam's construction and accordingly preparation of the project's shop drawings. The dam has been designed as a RCC dam having three capped spillways, a water intake structure for the energy tunnel and two orifice spillways on the body. Additionally, it was considered that until the completion of Laleli and İspir dams, the sediment amount accumulated in the reservoir would exceed the Güllübağ Dam's dead storage volume with ease and designing two large capacity sluice gates is a must-done step. The fact that the entire volume of the reservoir is already 15 million m^3 shows the necessity of this consideration.

In this regard, the designer had asked for hydraulics model experiments in order to determine the project criteria in detail. Thus, a series of experiments was conducted to obtain including not only experiments on the spillways but also on the sediment sluice gates/sluice gates, which is the part what this study focuses on.

The study is basically the analysis of the data obtained during the experiments. Firstly, the related reservoir area is gridded as 9x5x5m in three dimensions, the velocity values measured in three directions, x, y and z on 225 different grid points in total at five different levels, so each level has its own 45 measurement points. The velocity data is inherently in the form of time series and the analysis consists of several phases beginning with using these time series. Velocity time series have allowed us to calculate the average velocity values and then the turbulent fluctuation components for each point. Afterwards, non-dimensional turbulent shear stresses have been found by the fluctuation components to lead up to do the analysis in a more convenient way because the analysis would not mean much if those values were dimensional. In other saying, dimensional values depend on the magnitude whereas the non-dimensional ones do not.

Within the scope of the analysis, a few visualization works are prepared as well. The resultant vectors of average velocities are plotted in 2D and 3D by using MATLAB just like the first steps of analysis, in order to observe the vectors' directional trend and to see whether the vectors move into the sluice gates. Besides, the non-dimensional shear stress values are plotted in 2D as contour maps in the software called Surfer in order to detect the most-stressed zones and subsequently the stress values and contour maps are together examined to be associated with the grain diameter by the Shields parameter; by this way, it is possible to know where the sediment accumulation will likely occur and which zone permits how large sediment to move since it is a function of the shear stresses. Moreover, an approach suggested by other scientists who worked in the related field, the scour cone volume and length, which develops after flushing is used to see whether the approach is comparable with the laboratory data. Finally, the conclusions and recommendations are shared in the last chapter. Besides, the mentioned series of experiments done years ago are not a part of this study.

AÇIK KANALDAKİ REYNOLDS GERİLMELERİNİN SEDİMENT YIKAMA İŞLEMİ SIRASINDA DEĞERLENDİRİLMESİ

ÖZET

Rezervuar kapasitesinin belirlenmesi her zaman baraj tasarım süreçlerinin önemli bir parçası olmuştur. Bir rezervuarın kapasitesi, "Kütle Eğrisi Analizi", "Sıralı Pik Analizi" ve "Operasyon Çalışması" gibi bazı yöntemler kullanılarak hesaplanır. Barajın ölü hacim değeri, bazı ampirik formüller kullanılarak yıllık sediment birikiminin tahmin edilmesi ile ardından ise yüzdesel olarak ifade edilen rezervuar verimliliğinin tahmin edilmesiyle elde edilir. Verimlilik, rezervuar kapasitesinin toplam debiye oranının bir fonksiyonu olarak da tanımlanabilir. Genelde sediment birikimi, rezervuara giren debinin büyüklüğüne bağlı olarak düşük miktarlardan büyük miktarlara kadar değişebildiğinden, sediment birikiminin tahmin edilmesi zordur ve hesaplanan ölü hacim değerleri gelecekte karşılaşılması muhtemel gerçek değerleri yansıtmayabilir. Bu tür yanlış tahminler, beklenmeyen ve ekstrem boyutta olan sediment birikiminden dolayı barajın tahmini kapasitede işletilememesi nedeniyle büyük mali kayıplara neden olmaktadır. Rezervuar kapasitelerini yeniden kazanmak için, dünyada kullanılan en yaygın teknik olan boşaltma, sifonlama, tarama ve yıkama gibi bazı teknikler uygulanır. Ayrıca, bütün nehir havzasının işletimindeki birkaç düzensizlik de beklenmedik miktarda sediment birikimine neden olabilir. Örneğin, havzada bulunan öncelikli bir barajın inşaatına başlanması gerekirken havza planını da bozarak ikincil bir barajın inşaatına başlamak bu usulsüzlüklerden biridir. Çalışmamıza sebebiyet veren durum da benzer bir yanlışlıktan kaynaklanmaktadır.

Laleli, İspir ve Güllübağ barajlarının debi ve hız anlamında dünyanın en büyük nehirlerinden biri olan Çoruh nehrinin ana koluna yapılması planlanmıştır. Nehrin debisi yıldan yıla değişmekle birlikte, genellikle 200 m^3/s'nin üzerinde bir ortalama debiye sahiptir. Tüm bu üç barajın da Çoruh havzasında hem su potansiyeli hem de sediment birikiminin düzenlenmesinde kilit rol oynaması beklenmiştir. Bu bağlamda, sırasıyla Laleli, İspir ve Güllübağ barajlarının yatırıma dönüştürülmesi gerekiyordu. Ancak bazı finansal nedenlerden dolayı ilk olarak Güllübağ Barajı inşaatına başlanması ve buna bağlı olarak projenin uygulama projelerinin hazırlanmasına karar verilmiştir. Baraj, üç kapaklı dolu savağa, enerji tüneli için bir su giriş yapısına ve gövdede iki adet sediment savağına sahip olan bir silindirle sıkıştırılmış beton baraj olarak tasarlanmıştır. Bunlara ek olarak, Laleli ve İspir barajlarının tamamlanmasına kadar, rezervuarda biriken sediment miktarının Güllübağ Barajı'ndaki ölü depolama hacmini kolaylıkla aşacağı ve iki büyük kapasiteli sediment savağı tasarlamanın elzem bir adım olduğu düşünülmüştür. Rezervuarın toplam hacminin 15 milyon m^3 olması, bu düşüncenin gerekliliğini göstermektedir.

Bu kapsamda tasarımcı firma, proje kriterlerini detaylı olarak belirlemek için Istanbul Teknik Üniversitesi Hidrolik Laboratuvarı'ndan hidrolik model deneyleri talep etmiş ve bu kapsamda sadece dolu savak deneyleri değil, aynı zamanda bu çalışmanın da

odak konusu olan bir dizi sediment savağı deneyi de gerçekleştirilmiştir. Sediment savağı deneylerinden bu çalışmayı ilgilendiren kısım modelin oluşturulması, malzeme seçimi gibi temel adımların yanında, hız-basınç profillerinin elde edilmesi ve yıkama deneylerinin yapılmasıdır. Analiz bölümünde, bu deney adımlarında elde edilen veriler yorumlanacak ve bu ölçülen değerlerden yola çıkarak gerekli hesaplamalar gerçekleştirilecektir.

Çalışma kapsamında, giriş kısmında tezin ana başlıklarından ve belli başlı içeriklerinden sırasıyla bahsedilmiş, çalışmayı inceleyecekler için genel bir bakış açısı kazandırmak amaçlanmıştır. Hâlihazırda yapılmış olan sediment savağı deneyleri ve bu deneylerden elde edilen veriler doğrultusunda hazırlanmış analizlerden önce, konu ile ilgili dünya genelinde yürütülmüş çalışmalar aktarılmıştır.

Çalışmada yapılan sediment savağı deneyleri, temel fiziksel büyüklüklerin ölçeğinin belirlenmesini de kapsayacak şekilde deneye hazırlık sürecinden başlayarak ve deney sonuçlarından da kısaca bahsedilerek irdelenmiştir. Deneye hazırlık kısmında model/prototip ölçeklerinin belirlenmesi, deney alanının tespit edilmesi ve modelde kullanılacak malzeme seçimi gibi olgular aktarılmıştır.

Çalışma esas olarak deneyler sırasında elde edilen verilerin analizidir. İlk olarak, analizlerin temelini oluşturan mekanik bulgular paylaşılmış konunun fiziği ve temel denklemler ifade edilmiştir. Deney sırasında ilgili rezervuar alanı üç boyutta 9x5x5m olarak gridlenmiş, üç farklı yönde de ölçülen hız değerleri, toplamda beş farklı seviyede ve 225 farklı noktada x, y ve z hızları olarak adlandırılmak suretiyle ölçülmüştü. Analiz, zaman serileri biçiminde olan hız-zaman serileri kullanılarak başlar ve ileriki aşamalara geçer. Hız-zaman serileri, ortalama hız değerlerini ve ardından her nokta için analizi daha anlamlı kılmak adına kritik kayma hızı değeri ve türbülans çalkantı bileşenleri kullanılarak boyutsuz kayma gerilme değerleri bulunmuştur. Bu boyutsuz gerilmelerin her bir kotta yani 5 farklı seviyede eş-gerilme eğrileri SURFER adlı programda oluşturulmuştur. Bu çalışma, boyutlu büyüklüklerle yapılsa idi çok anlamlı olmayabilirdi. Bir başka deyişle, boyutlu değerler büyüklüğe bağlıyken boyutsuzlar değildir ve farklı ölçekteki benzer senaryolar için de geçerli olabilirler.

Analiz kapsamında eş-gerilme eğrilerinin yanında başka görsellere de yer verilmiştir. Deneylerden elde edilen üç yöndeki akım hız vektörleri her bir kot için 2B olarak çizdirilmiş; bileşke hız vektörlerinin büyüklükleri irdelenmiştir. Bunun yanında, vektörlerin yönünün sediment savaklarına doğru olup olmadığı da bu vektör çizimi ile anlaşılmıştır. Vektörlerin üç boyutta bileşkesi de alınarak elde edilen vektörler 3B olarak yine MATLAB kullanılarak çizdirilmiştir. Bu görseller, rezervuardaki akımın karakteristiğini, türbülans çalkantı bileşenlerini, kayma gerilmelerini ve dolayısıyla yıkama sırasındaki türbülans etkisini anlamada temel oluşturmuştur. Analize başlarken boyut analizi yapılmış, hadiseye etki eden parametreler paylaşılmıştır. Analiz sonuçlarından sonra, bu alanda çalışan diğer bilim insanları tarafından önerilen, rezervuarda yıkama işleminden sonra gelişen oyulma konisi hacmini ve uzunluğunu tespit etmek amacıyla kullanılmış denklemler çalışmamız kapsamında incelenmiş, laboratuvarda elde edilen oyulma hacim ve uzunluk değerleri ile karşılaştırılmıştır. Shields kriteri kullanılarak kayma gerilmeleri ile sediment çapı arasında bağ kurulabilmiş rezervuardaki hareket ettirilebilecek dane çapı tespit edilmiştir. Shields' parametresinin kayma gerilmesinin bir fonksiyonu olmasından dolayı sediment birikiminin nerede olacağını ve hangi bölgenin ne kadar büyüklükte bir sediment

hareketine izin verdiğini bilmek mümkündür. Dahası, bu alanda çalışan diğer bilim insanları tarafından önerilen, rezervuarda yıkama işleminden sonra gelişen oyulma konisi hacmini ve uzunluğunu tespit etmek amacıyla kullanılmış denklemler çalışmamız kapsamında incelenmiş, laboratuvarda elde edilen oyulma hacim ve uzunluk değerleri ile karşılaştırılmıştır.

En son kısımda ise hâlihazırda yapılmış olan deneylerin verileri ışığında gerçekleştirilen bu analiz serisinin sonuçlarından bahsedilmiştir. Çalışmanın sonucunda elde edilen bilgiler ve öneriler sunulmuştur. Sonuç olarak, yapılan çalışmanın benzerlerine göre daha kompleks bir geometride yıkama işlemini değerlendiriyor oluşu gerçeğine rağmen çalışma kapsamında, analiz kısmında görülecek olan belli başlı fiziksel büyüklükleri hesaplamak için önerilen denklemler ile uyumlu sonuçlara varılmıştır. Ayrıca, basınçlı akım ile yıkama işlemi hakkında elde edilen genel kanılar paylaşılmıştır. Yapılan deneyler bu çalışmadan yıllar önce yapılmış olup bu çalışma kapsamında değildir.

1. INTRODUCTION

1.1 Definition of Problem

At the present time, sustaining the storage capacity of existing reservoirs grows in importance because building new reservoirs is quite difficult due to stricter environmental regulations, high costs of construction and lack of suitable dam sites.

Certain deficiencies in design, construction or operation process might cause decrease in storage capacity which means not to be able to fully utilize the reservoir. It has been revealed by some researchers, in the Draft ICOLD Bulletin (2009) that in world reservoirs, on average for a 35 years old dam, the accumulated sediment storage has been evaluated as 2000 million m^3, which is a huge amount and it is thus costly to remove that amount of sediment from a reservoir. The reason of the loss is mostly due to sediment accumulation, which is currently a popular research topic worldwide.

In our case, the construction of Güllübağ dam located in Çoruh river basin was decided to get started before the other two dams called İspir and Laleli which were also going to be built in the same river and whose construction processes were supposed to get started before Güllübağ's. This decision taken by the official authorities brought about a few issues including the problematic of this study, increasing in the expected sediment accumulation amount of Güllübağ reservoir perceptibly. In the light of these information, two high capacity orifice spillways had been planned to flush the sediment out considering the sediment was going to fill the reservoir within 4 years, which is a very short period for a dam aimed to have 50 years of economic life.

According to the degree of reservoir level drawdown near the sluicegate, flushing operation can occur in two ways: pressurized flow (or orifice flow) and free-surface flow. The configuration and amount of deposits in a reservoir depend on the characteristics of the reservoir operations, incoming sediment-water discharges, sediment properties, and reservoir geometry. Under the pressurized flow condition, a flushing cone in the vicinity of the sluice gate could be formed with wedge-shaped

deposition. If the water level is allowed to be drawn down, two types of erosion patterns can occur: progressive erosion and retrogressive erosion. Numerous reservoirs in different parts of the world have accumulated significant amounts of sediments, thus reducing the performance of reservoirs. The techniques for reservoir desiltation have received increasing attention recently. The control of reservoir sedimentation through hydraulic flushing has been successfully employed in the field to preserve the useful life of the reservoir.

If drawdown flushing is operated with wedge-shaped deposition, sediment deposits can be scoured in the vicinity of the sluicegate opening within a very short period of time under pressurized flow condition, and a funnel-shaped crater called flushing cone will be formed by the flushing flow according to Moghadam, Emamgholizadeh, Bina and Ghomeshi (2006) Once the flushing cone has been formed and there is no sediment moving into the cone, the water flowing through the opening is clear, that is, the formation of flushing cone is fairly stable, and no sediment will be removed from the flushing cone afterwards. If the water surface can be drawdown significantly to generate high flow velocity near sluicing outlet, the flowing water will start to erode the rim of the flushing cone and retrogressive erosion can occur.

In this study, the laboratory data, obtained when the experiments on the spillways and sluice gates of Güllübağ Dam were carried out in 2009 are used in order to examine the velocity of the flow in three directions and the shear stress values which needed to be raised to have a pressurized flow characteristic and accordingly the turbulence effect for the flushing process. Besides, at the end the results of the analysis are evaluated, and some suggested formulas are used to see whether those equations are applicable in the case of the present study.

1.2 Scope of Study

Firstly, the studies conducted in the related field were reviewed. In this context, the significant works made world-wide were presented. Secondly, hydraulics of the subject, namely pressurized flow and therefore the physics of the turbulence were explained in order to establish a ground for presenting of the study. Thirdly, the premade sluicegate experiments, whose data are used to actualize this study were briefly presented. The fourth focus of the study was to demonstrate the series of analysis made through the measured data and to compare the measured data in the

laboratory with the calculated data obtained using a few suggested equations and criterions in the meaning of scour cone analysis and motion of sediment. Lastly, the evaluations and suggestions on the present work were stated to conclude the study and to give a beneficial basis for the future studies in the relevant subject.

Moreover, there are two crucial difference between this study and the previous ones. To begin with, as it will be explained in the next chapter, Literature Review, even though most of the studies in this particular subject were conducted by using one-dimensional analysis and merely a few of these studies were made in two-dimensional, the present study is in three-dimensional. Secondly, this study has the aim of defining flow characteristics of sediment flushing region by means of velocity measurements and shear stress analysis based on 225 different points rather than average values.

2. LITERATURE REVIEW

To utilize flow to remove previous reservoir sediment deposit and to pass flow, in which the heavy sediment is predominant when the high flow occurs are two main types of flushing processes as stated by Shen and Lai (1996). Flushing process eventuates in only a local flushing cone and thus cannot be considered as an effective process when the level of water is high as displayed in Figure 2.1.

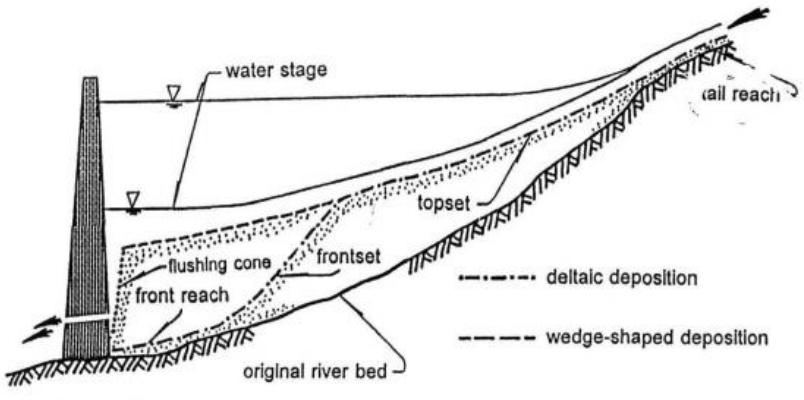

Figure 2.1 : Sketch of depositional patterns in profile.

Yet, when the topset of sediment deposit is very close to the water surface, in other

words when the level of water is low, the flushing process can be efficient in the meaning of both removing the accumulated sediment deposit and passing sediment in the flow if the frontset of the deposit has notably approached to a location very close to the dam. This happening, known as drawdown flushing, may bring about retrogressive erosion. As shown in Figure 2.2, especially for wide reservoir, a flushing channel generally occurs during drawdown flushing. In beginning, the top of the flushing flow is above the top of the flushing flow outlet and the flushing efficiency is not high enough within this period. Nonetheless, as the top of the flushing flow gets below the top of the flushing flow outlet, open channel flow occurs for the flushing flow; so that, the flushing efficiency increases considerably.

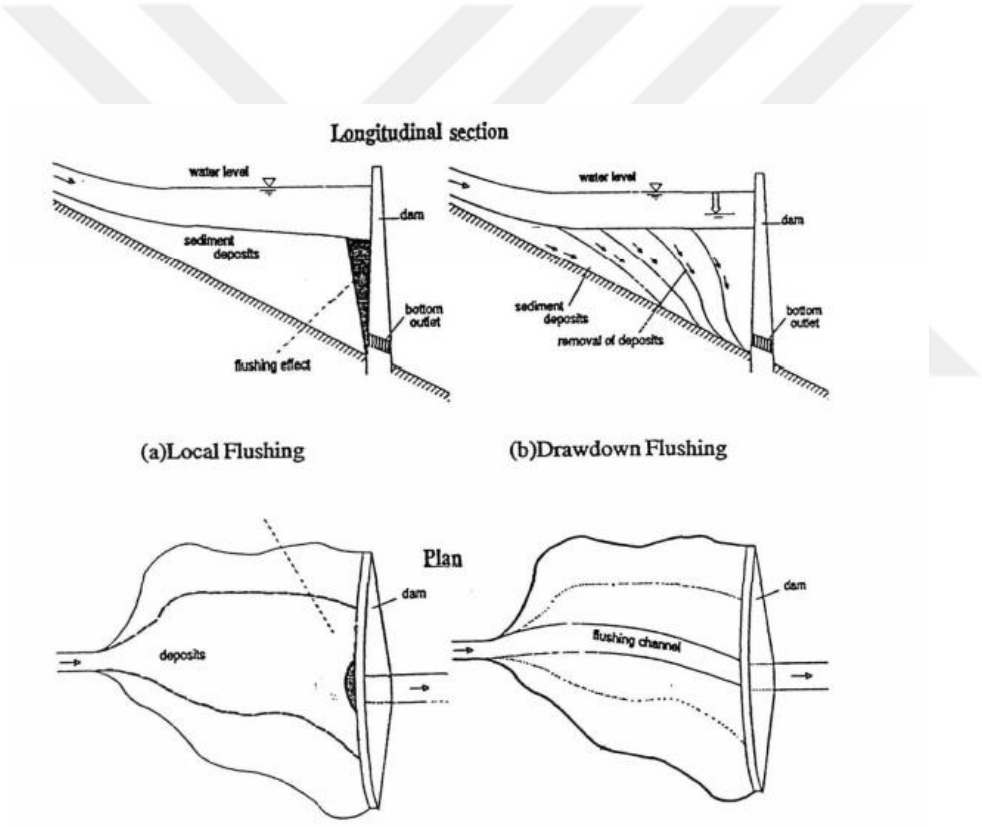

Figure 2.2: Sediment erosion.

The Tsinghwa University and Northwest Institute of Hydrotechnical Research (1979) and Lai and Shen (1996) demonstrated that relationship between flow characteristics in the flushing channel for field and laboratory data and sediment outflow can be evaluated by three curves for different sediment sizes as shown in Figure 2.3

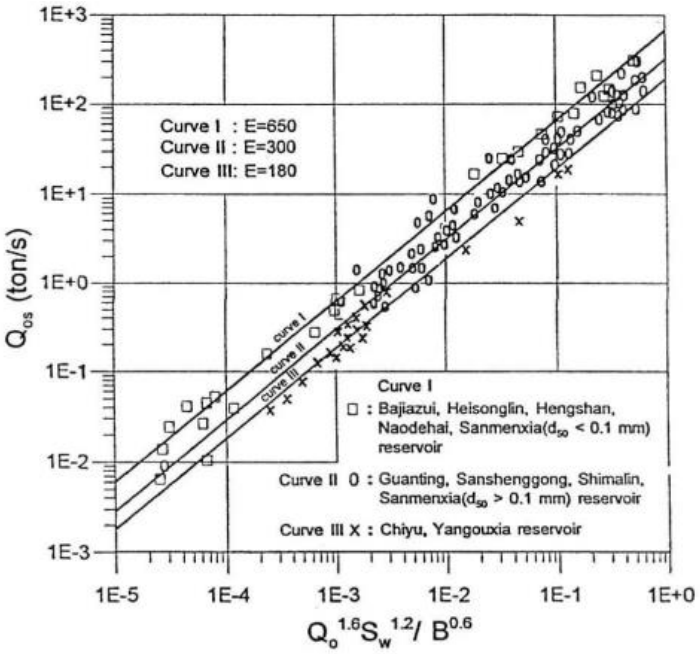

Figure 2.3 : Relationship between sediment outflow and flow characteristics in reservoir (after Tsinghwa University and Northwest Lab., 1979).

Janssen (1999) expressed that this relationship is applicable to not only steady flows but also unsteady flows. Presumably, other curves might exist for large sediment sizes, sediment that consists of cohesive material and that is for sediment deposit emerged over the water surface. Sediment outflow dramatically drops for pressurized flushing flow than that for open channel flows by way of the flushing flow outlet, as displayed in Figure 2.4.

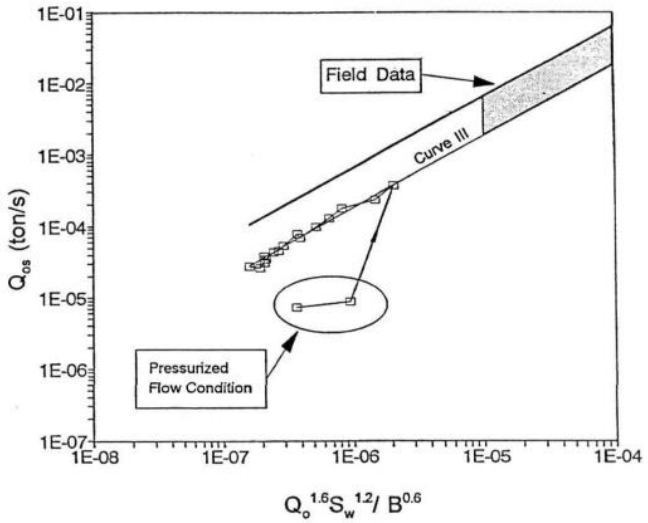

Figure 2.4 : Sediment outflow and flow characteristics from Lab. data (after Lai and Shen, 1996).

The existence of a flushing channel ought to be considered most especially for a wide

reservoir, if a numerical model is wished to use in order to analyze the flushing flow. As Lai and Shen (1996), and Atkinson (1996) indicated that flushing channel width, namely B can be taken as a function of the square root of the flow discharge which is the bankfull flow discharge of the flushing channel. This is basically a geomorphic relationship approximation, which is derived by both field and laboratory data and is very close to the regime relationship enhanced by Lacey (1931) from regime theory. The relevant relationship is displayed in Figure 2.5.

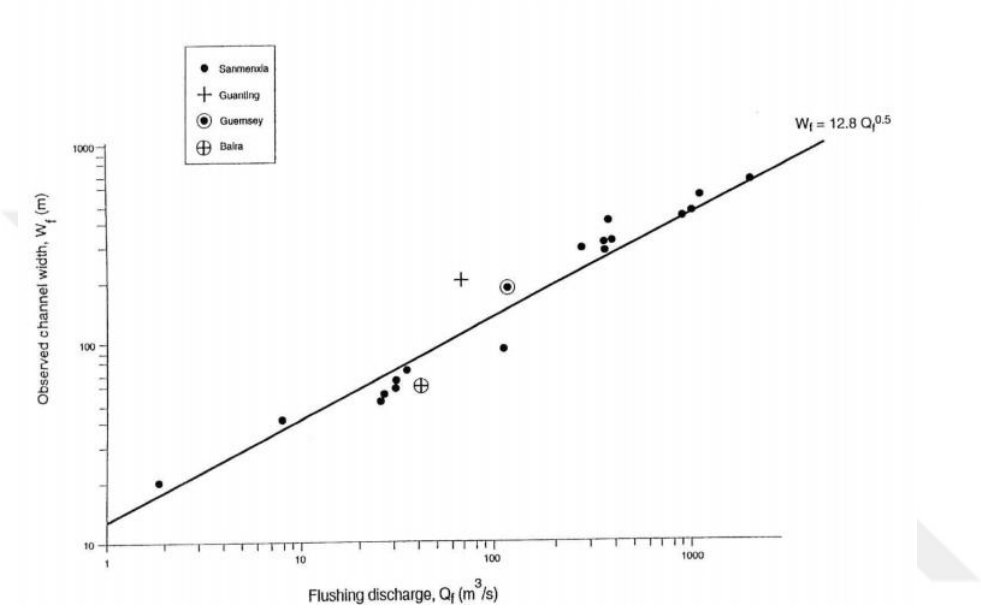

Figure 2.5 : Widths formed in reservoir deposits by flushing flows after Atkinson (1996).

The information given above must be used very cautiously. The Figure 2.4 can only be used when the sediment deposit is at a very close location to the dam and is in the form of the wedged type. The sediment outflow can be quite less than that shown in Figure 2.4, when the frontset of the reservoir sediment deposit is located far upstream from the dam. It can be stated that the distant the occurred deposit to the dam, the harder the flushing process. If the sediment deposit comprises cohesive material, the sediment outflow significantly decreases. According to Atkinson (1996), in the field cases, the sediment outflow was mostly much less than the outflow shown by Figure 2.4. In these field cases, the sediment deposit is most likely away from the dam and the efficiency of flushing process is hence not high. In addition to this possibility, the efficiency could be low due to the fact that the flushing period were too long. Many studies have been made relating to the problems of sediment flushing through

reservoirs; yet, most of these investigations are not easy to find since the results of these studies are commonly notified in engineering reports. IRTCES (1985), Albertson (1996) and Shen (1999) presented a broad analysis of flushing sediments by many authors. Some certain flushing sediment operations made in the fields (After Atkinson, 1996) are shown in the Table 2.1. Chinese engineers have remarkable experience with both sediment- pass-through and hydraulic flushing. They have utilized many mathematical and physical models to analyze the flushing sediment through Three Gorge Dam on the Yantze River. As Shen (1999) expressed, a very extensive amount of data has been hereby acquired by the Chinese in the field. In this context, it can be expressed the fact that to reach their data is not very possible as they do not simply share their experience with the rest of the world diminishes the significance of the related data collected by them for now. Nevertheless, field experience on reservoir drawdown flushing in China have been presented by IRTCES (1985), Ding and Long (1985), Shuyou (1988), Guohan and Zhenqui (1989) , Guan (1991), Zhang (1995), Fan and Fan (1996) and Zhang (1996). Amini and Fouladi (1985) investigated the Sefidrud reservoir in Iran, Gvelsini and Shamaltzel (1971) studied reservoir flushing in USSR, Sen and Srivastava studied the flushing operation in India and Boucard (1996) worked on the mud-sliding from the banks and the resuspension of sediment in reservoirs. Because flushing operation in various reservoirs is complicated, it is not easy to obtain an inclusive rule that can be used for most of these reservoirs. Even so, some meaningful information can be made as follows: firstly, the level of water in reservoir must be drawn down in any case to ease the efficiency of flushing. Secondly, flushing process is definitely more effective in narrow reservoirs than the wide ones. Thirdly, a distinct flushing channel takes shape and retrogressive erosion happens inside the flushing channel when the width of the flushing outlets is much less than the reservoir's width. Sediment may be accumulated out of the width of this flushing channel formed. The final inference is that an approach to obtain the width of flushing channel was taken by Atkinson (1996) from the field data, by Lai and Shen (1996) and Janssen (1999) from laboratory data, considering the channel width as a coefficient of about 11 to 12 times the square root of the bankfull discharge inside the flushing channel. This relationship coheres with the "empirical regime formulae" presented by Yalin (1992).

Many numerical models mostly based on a one-dimensional modelling have been

utilized to study long term hydraulic flushing and sediment-pass-through operations. For narrow reservoirs, flushing channel's existence was generally ignored in the numerical analysis since the assumption was that the width of the flushing channel was almost the same as the reservoir width and valley width. A one-dimensional diffusion model, which is on the removed sediment volume and bed profile alters with constant discharge and channel width during fishing was used by Peng and Niu (1987) and Ju (1990). Han and Ho (1996) determined the equilibrium slope of the flushing channel as they analyzed the Three Gorge Reservoir in China. For wider reservoirs, the width of the flushing channel was indicated in the numerical model. Kitamura (1995), Ziegler and Nisbet (1995) and Chang(1996) presented these analyses. Not many two-dimensional models have been applied to flushing sediment processes. A two-dimensional model developed in order to define the flow and areal sediment deposit patterns for flow and sediment entering a reservoir was used and presented by Bechteler and Nujic (1996). Moreover, Lai (1994) presented a two-dimensional finite volume unsteady flow and sediment transport model to demonstrate flushing channel formation during flushing process. This is precisely a useful study although it is still needed to improve.

Reservoir	Country	Reference
Baira	India	Jaggi and Kashyap (1984)
Gebidem	Switzerland	Dawans et al (1982)
Gmund	Austria	Rienossl and Schnelle (1982)
Hengshan	China	IRTCES (1985)
Honglingjin	China	IRTCES (1985)
Mangahao	New Zealand	Jowett (1984)
Naodehai	China	IRTCES (1985)
Palagneda	Switzerland	Swiss Nat. Committee on Large Dams (1982)
Santo Domingo	Venezuela	Krumdiek and Chamot (1979)

Table 2.1 : Examples of the reservoirs flushed after Atkinson, 1996.

3. PREMADE SLUICEGATE EXPERIMENTS

A series of hydraulic model experiments had been conducted in Hydraulics Laboratory of ITU in 2009 at the request of the designer firm of the Güllübağ Dam Project, aiming to examine the subjects relevant to spillways and sluice gates and to determine the design criteria on them. The principal part that is concerning the present study is the sluice gate flushing experiments and in particular the examination of velocity and shear stress profiles as there were also some other researches on the sediment/sluice gates carried out for different purposes such as analyzing of the efficiency of the sluice gates' capacity, determining of the curve of sediment evacuation and examining of the height of sediment evacuation channels.

3.1 The Preparation of the Model

A few fundamental physical and hydraulic features of the Güllübağ Dam, which was planned to build through RCC method are given below:

3.1.1 Physical features

* The crest length of the dam = 90 m
* The height of the dam, from the talveg = 61.5 m
* Talveg level = 1090.0 m
* Crest level = 1151.5 m
* Water surface level (Normal condition) = 1047.0 m
* Water surface level (Exceptional/flood condition) = 1149.8 m
* The location of the spillways = on the body (at the right)
* The number of spillways = 3
* Total width of the spillways = 3x13 = 39 m
* Spillway level = 1151.50 m
* The location of the sluice gates = on the body (at the right)
* The number of sluice gates = 2
* The geometry of the sluice gates = rectangular cross-section
* Sluice gate cross-sectional dimensions = (2x3.50x2.5 m)

* Sluicegate intake level = 111.0 m

3.1.2 Hydraulic features

* Design discharge of the spillways = 3386 m^3/s

* Flood discharge of the spillways = 4464 m^3/s

* Design discharge of the sluice /sediment sluicegates = 431 m^3/s

* Design discharge of the tunnel =117 m^3/s

In the Hydraulics Laboratory of ITU, the place where the model was built has an area of 40x125 m and height of 9.50 m. Between the main water tank and the experiments systems, a pumping station, which has installed capacity of 450 kW, pressure head of 15 m and a capacity that is able to provide circulation flow of 600 lt/s is existing. The discharge value of 5012 m^3 (4.464+117+431=) is paid regard to determine the maximum geometrical model scale, while the physical dimensions of utilizable area in the laboratory is not considered in this matter. This value is obtained by calculating the sum of the maximum discharges in the spillways, sediment sluicegates and the energy tunnel.

3.2 The Determination of the Model Scale and Construction of the Model

3.2.1 The determination of the model scale

The model scale is determined based on the following criterions:

- To provide a turbulent flow as the flow is turbulent in the prototype

- To have a model scale as large as possible in order to ground on the Froude criterion, which is only based upon the principle of similarity in the inertial forces and the gravitational forces. Not Reynolds but Froude model is selected to use since the study is an open channel problem.

- To consider the limit values of the existing pumping station and circulation capacity.

- To ensure equal horizontal and vertical scales. In other words, to be based on the undistorted model.

Within this scope, the geometric scale determined for model and correspondingly the model-prototype scales for other physical quantities, which are found by using Froude similarity criteria are as follows:

(“m” denotes the quantity in the model and “p” denotes the quantity in the prototype.)

Model geometric scale:	$L_r=L_m/L_p=1/30$
Discharge scale:	$Q_r=Qm/Qp=(1/30)^{2.5}=1/4930$
Velocity scale:	$V_r=V_m/V_p=(1/30)^{0.5}=1/5.5$
Time scale:	$T_r=T_m/T_p=(1/30)^{0.5}=1/5.5$

3.2.2 The construction of the model

As it is notified in the chapter 3.2.1, the model scale is determined as 1/30 and an area of 20x50m is reserved for the series of experiments. The model included the riverbed throughout 150 m in prototype and the slopes at both right and left; hence, the effects of the reservoir topography in nature are not ignored. In the model area, a reinforced-concrete wall, acting as the boundary of the area was built.

The necessary cross-sections were created using the topographical map of the reservoir. The cross-sections created were placed in the right locations thus and so the required grading/levelling work for the riverbed and the slopes had been done by utilizing sand and concrete. The structures of the dam model, evacuation channel, the dam’s body, the intake structure of the energy tunnel, the control valves etc. were constructed by transparent Plexiglas material and correctly placed in the model.

In addition to these, an array of triangular gates at the outlets of each structure is placed to measure the discharge and an array of nanometers are used to measure the pressure head. Yet, these parameters are concerning the present study. The related structural features of the sluice gate are given in the Table 3.1 with the equivalent values in the model.

	Feature		In prototype	In model
SLUICE-GATE	Cross-sectional dimensions	:	b=3.50 m. h=2.50 m	0.117x0.083 m
	Number of Gates	:	2	2
	Discharge capacity (Normal Condition)	:	440 m^3/s	89.25 lt/s

Table 3.1 : The characteristics of the sluice gates.

3.3 The Model Experiment Process

At the sediment sluicegate, namely sluicegate side, ADV is utilized in order to measure the flow velocities in all the three directions, x,y and z. In the flushing experiments, a granular PVC material called polystyrene is used as the model material. Basic characteristics of this material are given under the next title.

3.3.1 Choosing the sediment material used and its basic characteristics

The sediment in nature, sand for instance, has a specific weight of 2.65 g/cm^3. As the model scale is determined as 1/30, the sediment to be used in the experiment must be scaled down 1/30 times. In this case, the experimental work should be done with a very fine material and this circumstance would prevent the flow from providing a turbulent environment and the condition, in which the bed material should go out of the viscous sublayer completely.

A much lighter material with a smaller sedimentation velocity has to be used due to those reasons, just specified in the previous paragraph. Hence, granular PVC material is chosen in order to optimize the fineness and the traceability during the experiment.

The material has a specific weight of 1.04 g/cm^3, dimensions of 2.3 x 2.3x (2.9~3.7) mm and the grain-size distribution of the material is shown in Figure 3.1. As seen in the Figure 3.1, the average nominal grain size of the material is 3.3 mm and the PVC material is ranging in size from 2.9 to 3.7 mm.

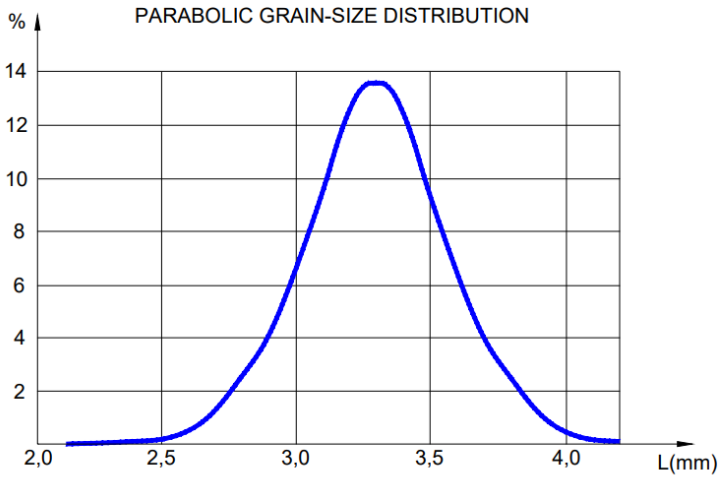

Figure 3.1 : Grain-size distribution of the PVC material used.

On the other hand, the sediment used in the model must satisfy the following equation to be in accord with the model similarity law.

$$L_s \times L_{\gamma s} = L_r$$

L_r is the geometrical scale of the model.

L_s is the geometrical scale of the sediment, $L_{sm}/L_{sp}=3/30$

$L_{\gamma s}$ is the specific weight scale of the sediment in water, equals to $\frac{1.04-1}{2.65-1} = 0.024$

Thereby,

$$L_s = \frac{D_m}{D_p} = \frac{L_r}{L_{\gamma s}} = \frac{1/30}{0.024} = 1.45 \qquad (3.1)$$

Because PVC is ranging in diameter from 2.9 to 3.7 mm, the equivalent grain size of the sand in nature is found as 2.0 ~ 2.6 by dividing the values by L_s, 1.45.

Principally, the maximum grain size that could be hazardous for the chosen turbine and the head of Güllübağ HPP is approximately 0.5 mm. Therefore, if the material equivalent to 2.6 mm in diameter can be flushed through the sluicegates in the model, it can be stated that the sluicegate is going to be dependably in service until a larger material load accumulates in long term.

3.3.2 Sluicegate flushing experiments

The images taken when conducting the sluicegate flushing experiments can be seen in the Figure 3.2, Figure 3.3, Figure 3.4 and Figure 3.5.

The experiments had been conducted under these conditions:

- The water surface level is at the normal condition,
- Energy tunnel is in service in a full capacity,
- Sediment/bottom gate valves are fully opened.

Almost the whole reservoir area, apart from a particular area located right in front of the sluicegate's intake is filled and leveled by the polystyrene material up to a certain elevation over the level of the sluicegate intake. Then, the valves of both the energy tunnel and the sluice gates are opened to observe the bed load sediment motion in the upstream of the dam (Figure 3.3).

Based on the same flow and service conditions, flow velocity values in three directions are measured at five different levels. Velocity vectors in 2D as one for each level and in 3D as one for the whole model are plotted. These plots (Figures 4.6- 4.11) are demonstrated in Chapter 4, Analysis Results and Discussions.

Figure 3.2 : Top view of the region near the dam embankment.

Figure 3.3 : Opening the two sediment sluicegates' and the energy tunnel's valves.

3.3.3 Comments on the sediment flushing experiments

Making the experiments on the sediment sluicegate flow conditions and the gates' structural efficiency provides the required data for the present study because the study mainly focuses on the velocity measurements done while there were no sediments in the model reservoir and therefore the pressurized flow and the flushing process as it is going to be explained step by step in the next chapter. After these experiments, a series of tests on the efficiency of flushing process and on determining the flushing capacity also were conducted. In the light of these tests, it can be expressed that in that kind of reservoirs, the large scaled sediment loads accumulate in the farthest upstream zone, in other words at the entrance of the reservoir and grain size of the accumulated sediment get smaller towards the body of the dam, in accordance with the mechanics of sediment accumulation.

Furthermore, in the regions close to the body where the flow area highly increases and thus the flow velocities decrease, a sediment accumulation having the characteristics of mud gets formed as the suspended load sediments gravitate towards the bottom of the basin by time. Although these suspended loads are fine enough to be evaluated as uncritical for the intake structure, these loads are considered as harmful for the reservoir as the accumulation gets formed by these loads will likely reduce the

reservoir capacity in progress of time.

In consideration of Güllübağ HPP's height of drop of 100 m, the grains with diameter of 0.6 mm or higher must not penetrate the tunnel via the intake and then the turbines via the tunnel. In other saying, the critical grain size is 0.6 mm as in diameter. Since the experiments were conducted by using PVC material as the bed load sediment, specific weight of 1.04 g/cm^3, it is possible to determine the flushing effectiveness of the sluicegate planned. For this reason, a certain zone between sediment sluicegate level and the tunnel intake's bottom level and throughout 2 m towards the upstream is filled by utilizing 1 m^3 of polystyrene (Figure 3.4). Then, a series of tests on the flushing efficiency of the gates are made at different water surface levels, 1147 m and 1133 m, at the maximum service level and at the top of the spillway crest while the valves are opened. Within the experiments based on the predefined flow and service characteristics, flow velocity profiles forming due to the spillway, tunnel and the sediment sluicegate currents are obtained. It is also detected that there is not much change between the two operation scenarios ("spillway, sediment sluicegate and the tunnel are in service" and "tunnel and the sediment sluicegate are in service"), in the meaning of both velocity directions and magnitudes. Unsurprisingly, the rate of velocity, reaching up to 1.00 m/s in front of the sediment sluicegate is rapidly decreasing towards the upstream.

Figure 3.4 : PVC material used during the experiment.

Figure 3.5 : Location of the model in the laboratory.

4. ANALYSIS RESULTS AND DISCUSSIONS

The turbulence effect, the pressurized flow characteristics need to be known to effectuate the pressure flushing process. This signifies the fact that the turbulent flow and its components must be extendedly investigated in order to analyze the process properly. As mentioned in the previous chapter, the measured values concerning the present study are velocities in three directions because the fluctuating velocity components are obtained by using the measured velocities and these components allows us to calculate the Reynolds stresses .Eventually, the Reynolds stresses provide to observe the potential motion of the sediment load and demonstrate whether the efficiency of the flushing is sufficient in the relevant regions. In this chapter, firstly, the mechanics of the subject is going to be examined step by step and then the analysis made by the experiment data, afterwards the results of the analyses and the discussions/comparisons regarding them are going to be presented. Furthermore, the Güllübağ HPP is an impoundment facility, where the water released from the reservoir

flows through a turbine and activates a generator to produce electricity .

4.1 The Mechanics of the Subject

As it was mentioned under the title 3.3.3, the velocity data that actualize this study were measured while there were no sediment in the model reservoir and the flow regime might be considered as free flow since the sediment gates' do not have any contact with water downstream unlike the submerged flow regime where the structure, in this case the gates, has contact with water both upstream and downstream.

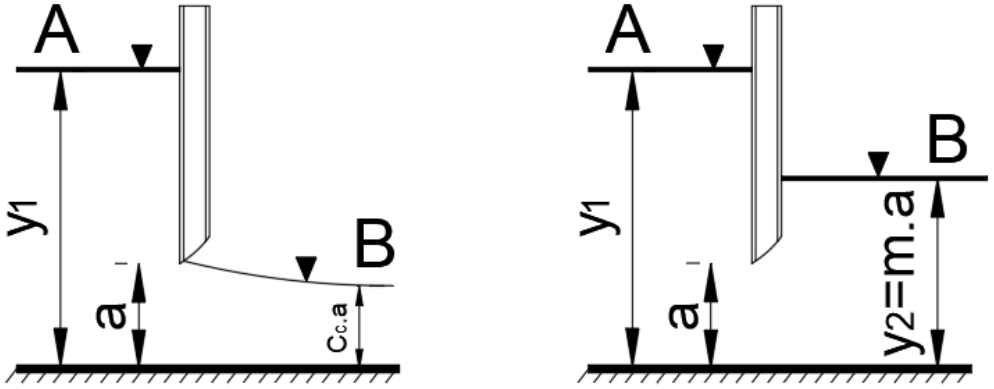

Figure 4.1 : Free and submerged flow regimes respectively.

4.1.1 Reynolds decomposition

Before starting to explain the analyses made, it is indispensable to discourse the mechanics of this subject by means of basic principles in order to make this study more comprehensible. The mean value of a hydrodynamic quantity, for instance x_i – component of the velocity u_i , is defined as follows:

$$\overline{u_i} = \frac{1}{T}\int_{t_0}^{t_0+t} u_i dt \tag{4.1}$$

In which, T is the total time of measurement, in other words the time spent to obtain the mean value and t_0 is any arbitrary time. T must be certainly large to get a reliable mean value. Time series of u_i is seen in Figure 4.2. Figure 4.3 and Figure 4.4 illustrate the time series of the velocity values and the power spectrum in x, y and z directions

at a point, called B24 (subject of "naming the points" is going to be covered under the title of "Presenting the grid system") in the present study. This is called time averaging, which is only one of the averaging methods, for example ensemble averaging, moving averaging etc. The instantaneous value of velocity u_i may be written as:

$$u_i = \overline{u_i} + u_i' \tag{4.2}$$

This is what the Reynolds decomposition; u_i' is the fluctuating part (or fluctuation) of u_i and $\overline{u_i}$ is the mean of u_i. The Reynolds decomposition can be applied to any hydrodynamic quantity and the time series of u_i can be observed in Figure 4.2.

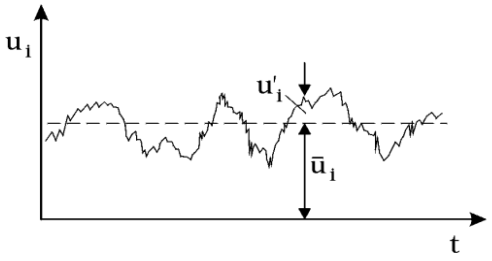

Figure 4.2 : Time series of u_i .

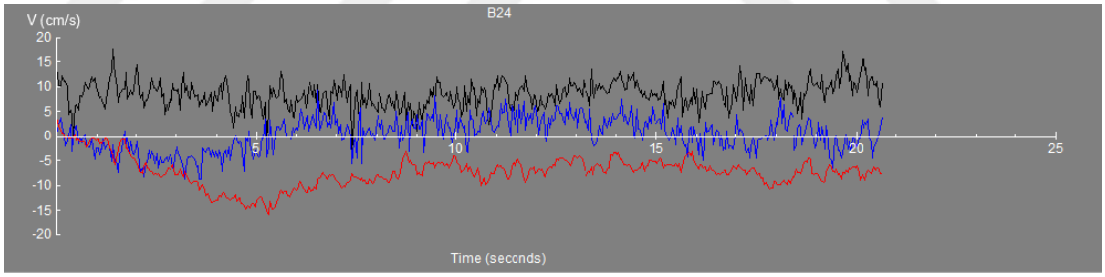

Figure 4.3 : Time series of u_i, v_i and w_i at the point B24.

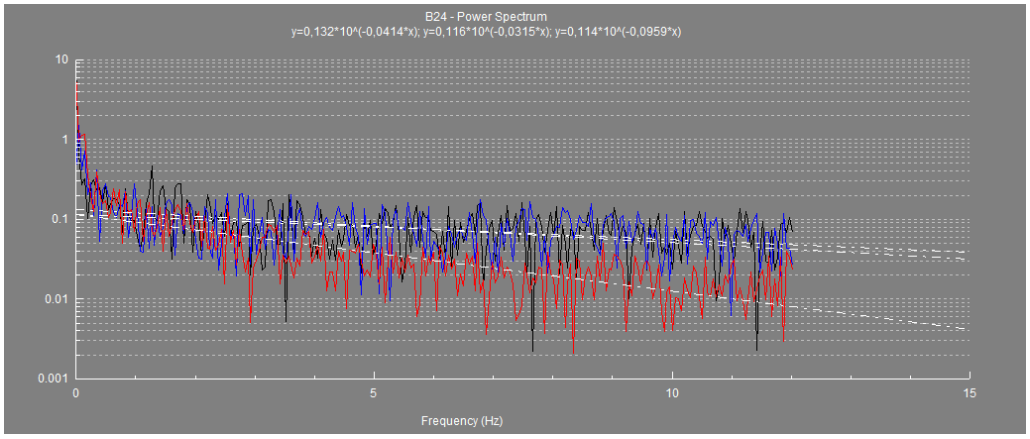

Figure 4.4 : Power spectrum at the point B24.

4.1.2 Conservation of mass

The continuity equation is derived from the conservation of mass, which counts as one of the fundamentals of fluid mechanics and it is given as follows for the incompressible fluids, for instance the water:

For incompressible fluids, for instance the water,

$$\frac{\partial u_i}{\partial x_i} = 0 \tag{4.3}$$

In which u_i is the the i- component of the velocity. Averaging the the mean value of the i- component:

$$\frac{\overline{\partial u_i}}{\partial x_i} = \frac{\partial \overline{u_i}}{\partial x_i} = 0 \tag{4.4}$$

Which can be defined as the continuity equation for the mean velocity and subtracting this equation from $\frac{\partial u_i}{\partial x_i} = 0$ gives

$$\frac{\partial u_i'}{\partial x_i} = 0 \tag{4.5}$$

Consequently, it can be stated that the equation just obtained above is the continuity equation for the fluctuating part.

4.1.3 Conservation of momentum and Reynolds stress

Navier-Stokes equations represent the conservation of momentum in fluids and are applied to study various dynamic or thermal interactions. For a Newtonian fluid, which is defined as the fluid with constant viscosity in which the shear rate is directly proportional to the shear stress, the Navier- Stokes equation is given as:

$$\rho\left(\frac{\partial u_i}{\partial t} + u_j \frac{\partial u_i}{\partial x_j}\right) = \rho g_i + \frac{\partial \sigma_{ij}}{\partial x_j} \tag{4.6}$$

Where,

t is the time,

g_i is the volume force, gravity force in this case,

x_i is the Cartesian coordinates and

the σ_{ij} is the stress tensor in the fluid and can be expressed as follows:

$$\sigma_{ij} = -\rho\delta_{ij} + \mu(\frac{\partial u_i}{\partial x_j} + u_j \frac{\partial u_j}{\partial x_i}) \tag{4.7}$$

The preceding equation is the constitutive equation for a Newtonian fluid and p is the pressure, μ is the viscosity and the δ_{ij} is the Kronecker's delta, which can be explained as:

$$\begin{aligned} \delta_{ij} &= 1 \text{ for } i = j, \\ \delta_{ij} &= 0 \text{ for } i \neq j \end{aligned} \tag{4.8}$$

If the Navier- Stokes equation is integrated with the continuity equation, the following equation can be written:

$$\rho(\frac{\partial u_i}{\partial t} + \frac{\partial}{\partial x_j}(\rho u_i u_j) = \rho g_i + \frac{\partial \sigma_{ij}}{\partial x_j} \tag{4.9}$$

By averaging each term in the previous equation and using Reynolds decomposition, the following equation, which is also known as Reynolds equation is obtained.

$$\rho(\frac{\partial \bar{u}_i}{\partial t} + \bar{u}_j \frac{\partial \bar{u}_i}{\partial x_j} = \rho \bar{g}_i + \frac{\partial}{\partial x_j}(\bar{\sigma}_{ij} - \rho\overline{u_i' u_j'}) \tag{4.10}$$

Here, the additional stresses $\rho\overline{u_i' u_j'}$ exist in the case of the turbulent flow as seen in the equation above. This additional stress is called Reynolds stress and these stresses generate a symmetrical second order tensor. In other words, there are nine such stresses and these can be displayed in a tensor form as:

$$-\rho\overline{u_i' u_j'} = \begin{bmatrix} -\rho\overline{u_1' u_1'} & -\rho\overline{u_1' u_2'} & -\rho\overline{u_1' u_3'} \\ -\rho\overline{u_2' u_1'} & -\rho\overline{u_2' u_2'} & -\rho\overline{u_2' u_3'} \\ -\rho\overline{u_3' u_1'} & -\rho\overline{u_3' u_2'} & -\rho\overline{u_3' u_3'} \end{bmatrix} \tag{4.11}$$

Consequently, at this point there are in total four equations for the mean flow: the continuity equation and the conservation of momentum, namely Navier-Stokes equations in three directions, x, y and z. On the other hand, there are ten unknowns($\overline{u_i'}$,three components of velocity, $\overline{\rho}$ pressure and $-\rho\overline{u_i'u_j'}$ six components of Reynolds stress) in the case of turbulent flow whereas there are four unknowns for laminar flow. This situation can be defined as equation deficiency in turbulent flow, also called the closure problem of turbulence.

4.2 The Dimensional Analysis

In a reservoir, generally after flushing process, it is natural to expect a scour cone volume and a length developing. The equilibrium of this development depends on a few parameters: depth H_w, which is defined as the reservoir water, depth of deposited sediment H_s above the intake, fluid density ρ_w, sediment density ρ_s, the characteristic length L, water velocity at intake u, fluid dynamic viscosity μ, gravitational acceleration g, and main grain diameter d_{50} of non-cohesive sediment. These parameters are separately expressed below:

$$V = f(u, H_w, H_s, L, g, \rho_s, \rho_w, d_{50}, \mu)$$
$$L = f(u, H_w, H_s, L, g, \rho_s, \rho_w, d_{50}, \mu) \quad (4.12)$$

In this study, L, the characteristic length for non-circular cross-sections, as a fact in hydraulics can be taken as 4R, which is four times the hydraulic radius; besides, the parameter $\rho_w uD$ is already negligible because in this study the flow worked with is turbulent as it is going to be calculated within the next paragraph. Re, the Reynolds number is the ratio between the inertial and viscous forces in a fluid and determines the characteristic of the flow, if the Reynolds number is higher than 4000.

$$\mathrm{Re} = \frac{uL}{\upsilon} \quad (4.13)$$

Where u is the velocity of the fluid (m/s), L is a characteristic length (m) and υ is the kinematic viscosity of the fluid (m^2/s). When considering the data related to the prototype, each of the two sluice gates has a width of 2.5 m and height of 3.5 m; in this way, the characteristic length can be calculated as:

$$D = 4R = 4\frac{A}{P} = \frac{4\times 2\times 3.5\times 2.5}{2\times 12} = 2{,}92\ \text{m} \qquad (4.14)$$

The experiment data shows that the resultant velocity values vary from 1 cm/s to 9 cm/s, the equivalent values in the nature would be respectively 0.055 m/s and 0.495 m/s as the velocity scale is 1/5.5. The kinematic viscosity of water can be taken as 1x 10^{-6} m^2/s.

$$\text{Re} = \frac{0.055\times 2.92}{1\times 10^{-6}} = 160600 > 4000 \qquad (4.15)$$

4.3 The Grid System and the Velocity Distribution in the Reservoir

4.3.1 Presenting the grid system

It was adverted that the reservoir is gridded to describe each measurement points' coordinates in horizontal plane and the levels in vertical. In this context, the points are named, and these named points (for the level 2, Z=1108 m in the prototype) can be seen in the Figure 4.5. By definition, there are five grid layouts in total as there are five measurement levels. The letter and the first number in the naming stand for the horizontal coordinates of the related point and the last following number represents the level. To set an example, the points C22 and E42 are shown in the Figure 4.5.

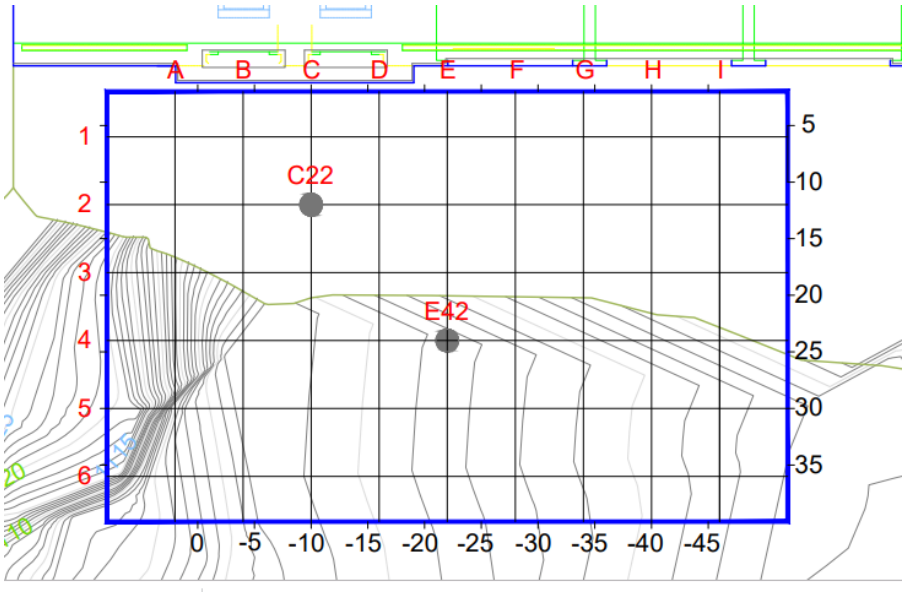

Figure 4.5 : The grid system and the naming described.

4.3.2 The velocity distribution in the reservoir near sluicegate

The $\overline{u_i'}$ values in three directions, obtained from the time series that consist of the data measured in the scope of the sluicegate experiments are plotted at each critical level, in terms of prototype, Z=1108m, Z=1110 m, Z=1111 m, Z=1113 m and Z=1118 m respectively. Z=1108 m represents the level 2 m below the sediment sluicegate intake, Z=1110 is the bottom level of the sediment sluicegate. Z=1111 m is the level of the sediment sluicegate mid-axis. Z=1113 m is the top level of the sediment sluicegate and finally Z=1118 m is 5 m above the top of the gate.

The vectors plotted are in fact the resultant magnitudes of the velocities at x and y directions range from 2 cm/s to 16 cm/s. The 2D plots indicates the velocity vectors' trend and demonstrates whether these vectors go towards the sediment sluicegates while the valves are opened under the normal service conditions.

In the zones close to the dam embankment, which is shown on each plot, the trend is as expected and towards the sediment sluicegates, drawn as red rectangles in the layout. However, the trend that the vectors follow is getting irregular and inordinate since the reservoir in nature, thus the test environment is not just a basic open channel with simple geometric characteristics. The complexity of the topography obviously gives rise to this sort of irregularities in the trend of the vectors.

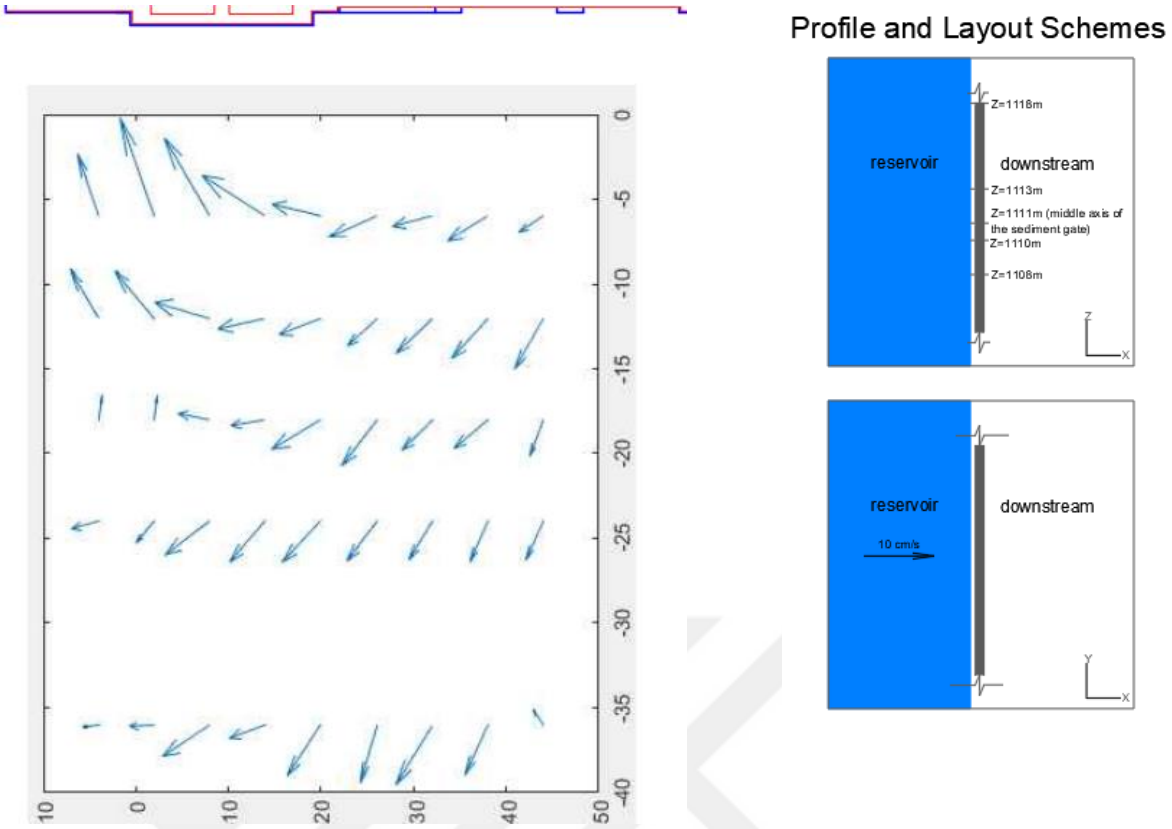

Figure 4.6 : The velocity vectors at Z=1108 m, 2 m below the sediment sluicegate intake.

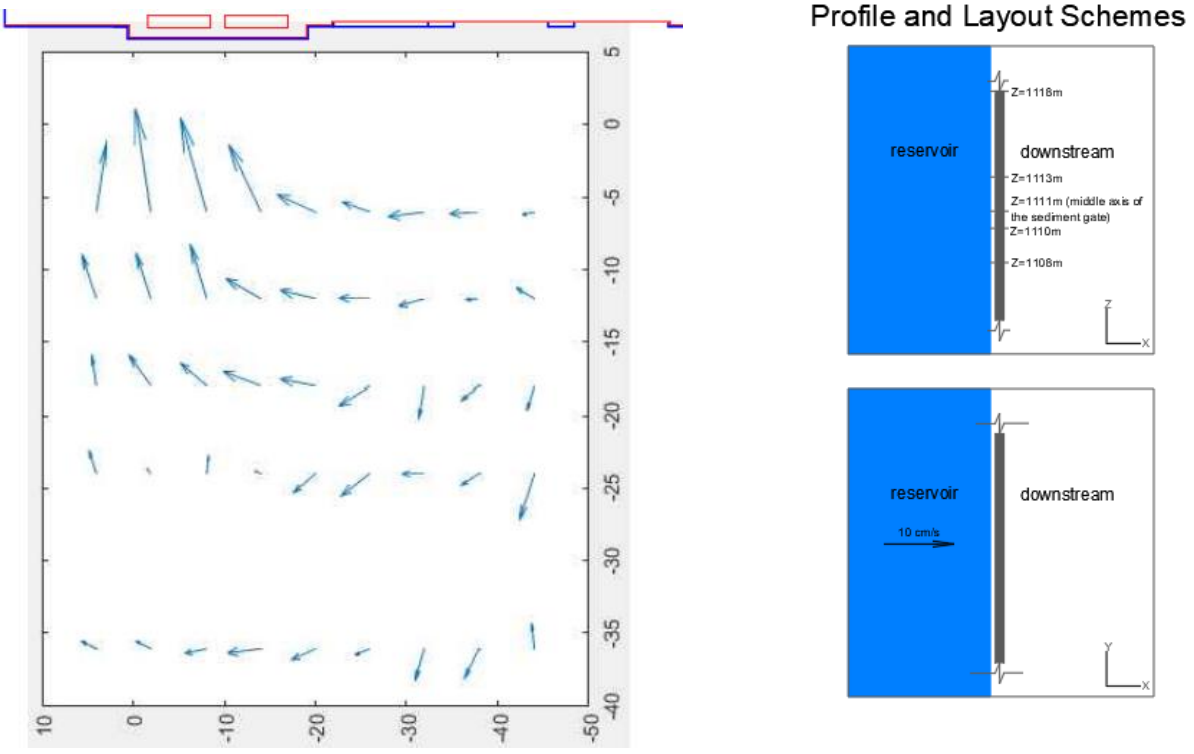

Figure 4.7 : The velocity vectors at Z=1110 m, bottom level of the sediment sluicegate.

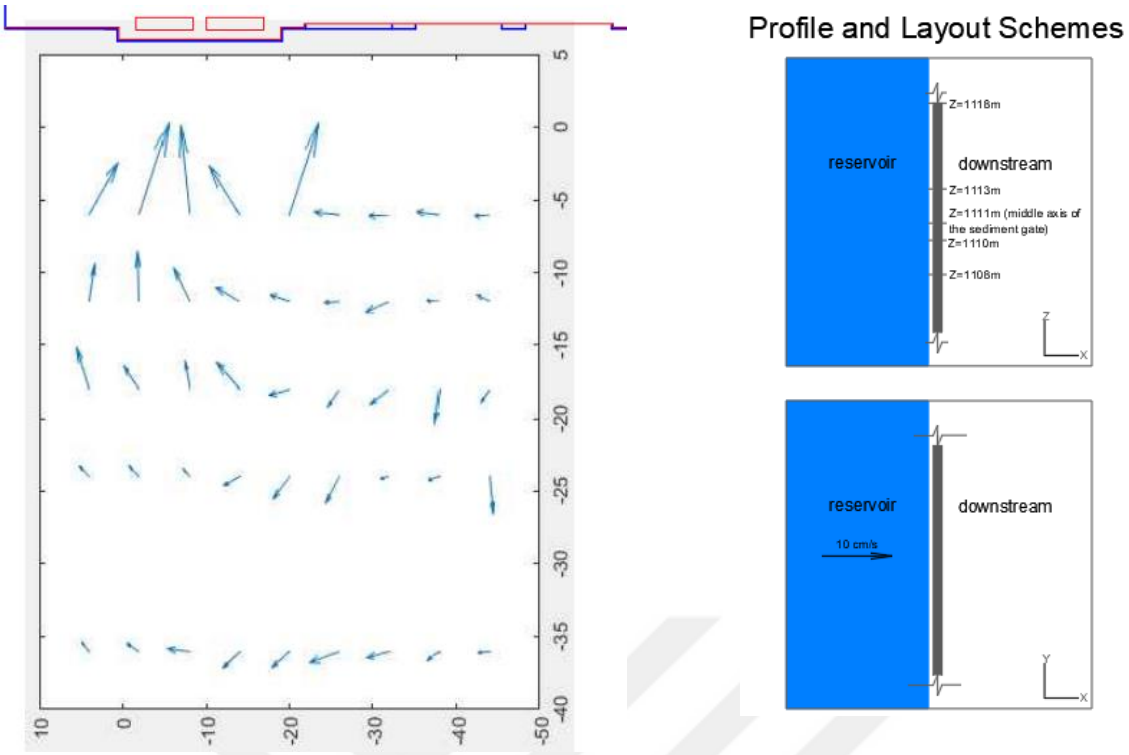

Figure 4.8 : The velocity vectors at Z=1111 m, the level of sediment sluicegate mid-axis.

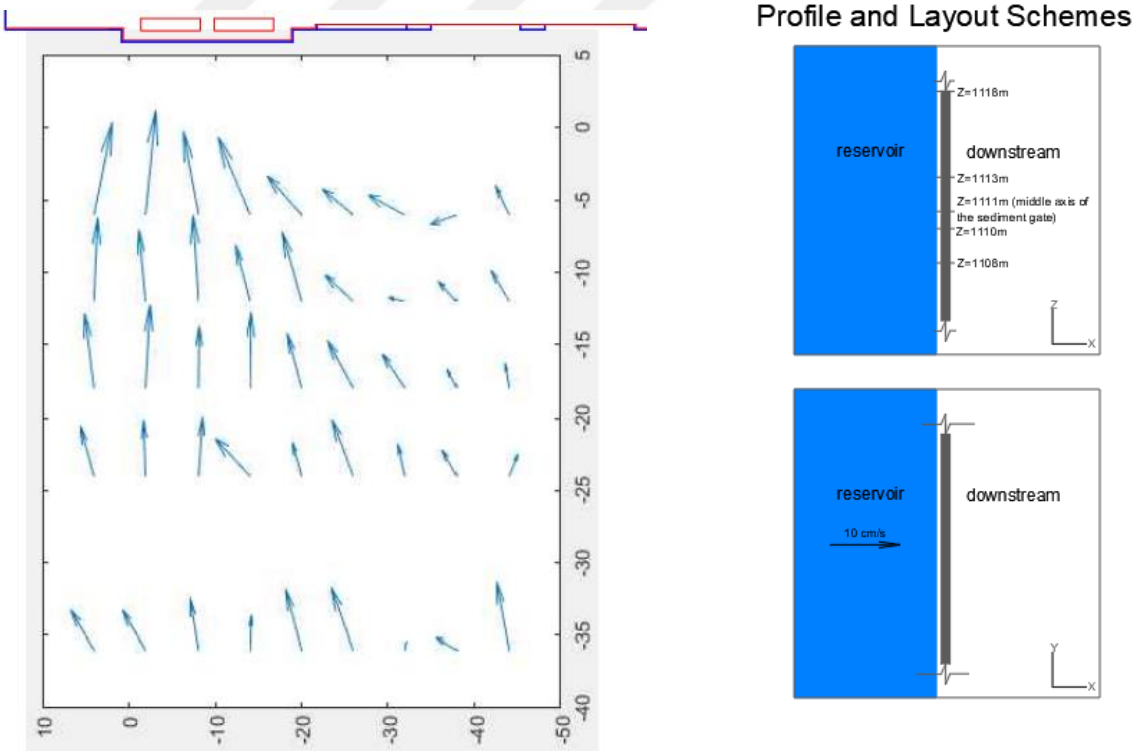

Figure 4.9 : The velocity vectors at Z=1113 m, the top level of the sediment sluicegate.

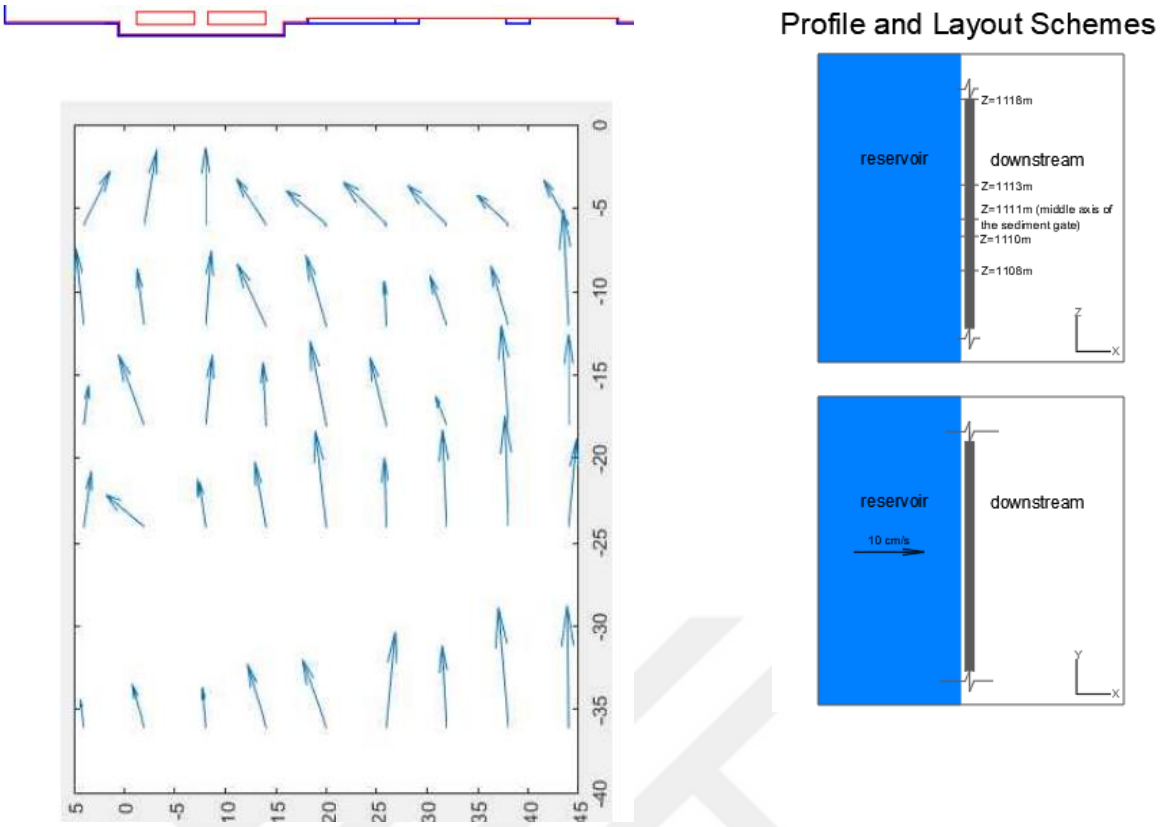

Figure 4.10 : The velocity vectors at Z=1118 m, 5 m above the top of the gate.

The velocity magnitudes are also determined in 3D and plotted as a 3D vector graph (Figure 4.11). Assuming the viewpoint is behind the dam embankment even though it is not possible to practice in nature, the view given below can be regarded as looking at the reservoir through a transparent embankment.

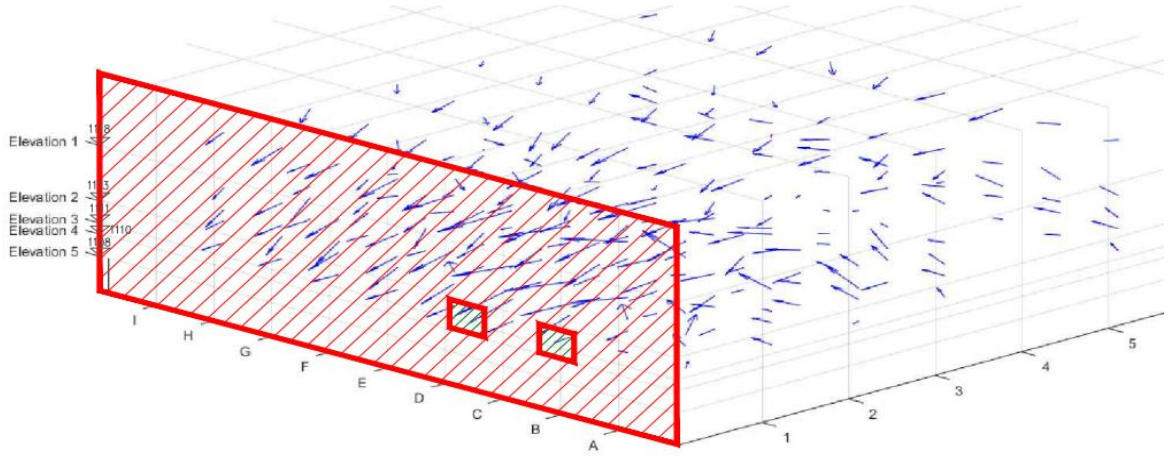

Figure 4.11 : The velocity vectors in 3D.

4.4 Determination of Reynolds Stresses

The reason why the present analysis is based on the Reynolds stresses is the fact that as getting away from the wall, the viscous part of the total shear stress is negligible and the turbulent part, namely Reynolds stresses can be thought as equal to the total shear stress, $\tau_0 = \tau_{turbulence}$. Figure 4.12 demonstrates the relation between the contribution of laminar and turbulent parts to the total shear stress as a function of the distance from the wall.

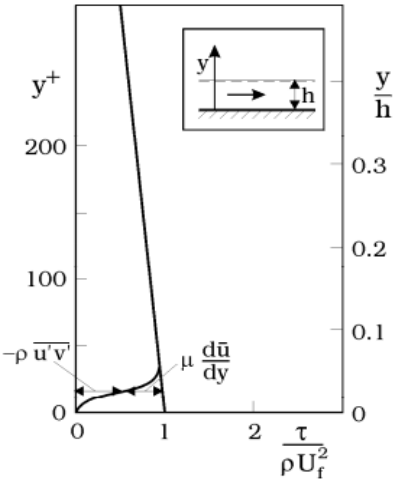

Figure 4.12 : The contribution of laminar and turbulent parts to the total shear stress (Grass,1971).

As it was mentioned while explaining the closure problem of turbulence, unlike the case of laminar flow, there are six additional unknowns: the six shear stresses shown in the Reynolds stress tensor. These stresses have been obtained by multiplying the specific weight with three different fluctuation components. These are respectively as follows:

$$-\rho\overline{u'w'},\ -\rho\overline{v'w'}\quad ,-\rho\overline{U_r'w'}$$

The velocity U_r is the resultant of u and v in horizontal plane. The only vertical one among these three velocity components, u, v and w is w. It can be above seen that the w is the irrevocable multiplier when determining the Reynolds stress since the shear stress occurs between two parallel horizontal planes in fluids just as in the solids. For instance, the friction when two sticks are rubbed together, may be pictured to comprehend the phenomenon.

In addition to this, in order to make the Reynolds stresses non-dimensional, the dimensional values had to be divided by another stress value; so that, the non-dimensional values would be more useful in analyzing the turbulence because the non-dimensional values make sense in the similar cases with different geometrical scales. The friction velocity could be determined to get this dividing term.

The friction velocity is found by a mean velocity profile throughout any vertical plane in the reservoir since the friction velocity U_f is determined by dividing the slope of the in semi-logarithmic velocity profile, tan α with the Von Karman constant, κ which is in general taken as 0.41 in fluids.

$$U_f = \frac{\tan \partial}{\kappa} \tag{4.16}$$

The time and space-averaged velocity near the bed satisfies the logarithmic law, which is expressed as

$$\frac{\langle \bar{u}(y) \rangle}{U_f} = \frac{1}{\kappa} \ln\left(\frac{30(y-\Delta y)}{k_s}\right) \tag{4.17}$$

The semi-logarithmic plot of the average u_i velocity's profile at a certain vertical plane is plotted below. Through C1 direction, by fitting the measured values exponentially, a line is obtained, and as it can be seen via the formula of the line, it intersects the y-axis at y=0.16 cm where $0.16 = \frac{k_s}{30}$. Thus, k_s, Nikuradse's equivalent sand roughness of the stones is equal to 4.8 cm.

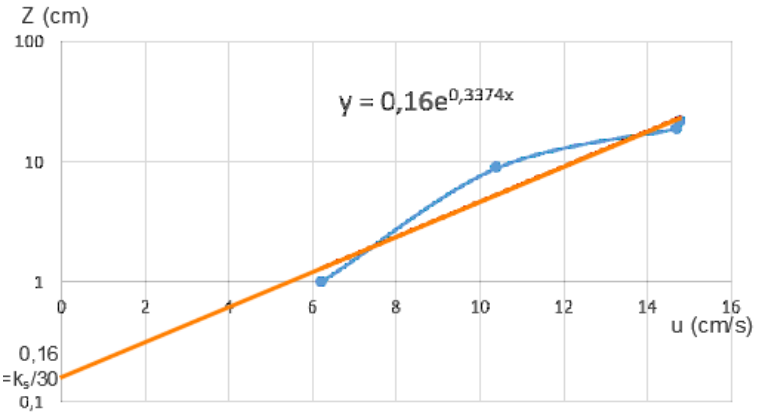

Figure 4.13 : Semi-logarithmic velocity profile through C1 direction to determine k_s.

As Sümer, Çokgör and Fredsøe pointed out in 2001, that k_s can be considered as follows:

$$k_s = (2-4)\,\mathrm{D} \tag{4.18}$$

As a result, $D = \frac{4.8}{2} = 2.4\,\mathrm{cm}$

The Von Karman constant is a dimensionless constant and as Orszag and Patera in 1981 summed up their work on Von Karman constant indicating that as the mean velocity profiles, Reynolds stresses and turbulence intensities are in accordance with the experiments they had conducted, the Von Karman constant is calculated to be $\kappa = 0.46 \pm 0.05$.

The C1 direction, which is a direction formed of the points C12, C13, C14, C15 and C16 is chosen as the critical vertical direction as this direction is close to not only the dam embankment and also the sediment sluicegates. The blue points in the plot represent the mean velocities in different levels; therefore, to make a line pass through these points would create a velocity profile in this direction. If the elevation values on the y axis are drawn in semi-logarithmic as the increment of the levels of the model are more suitable to do it and the velocities again in the model are plotted on the x axis, the following graph is obtained.

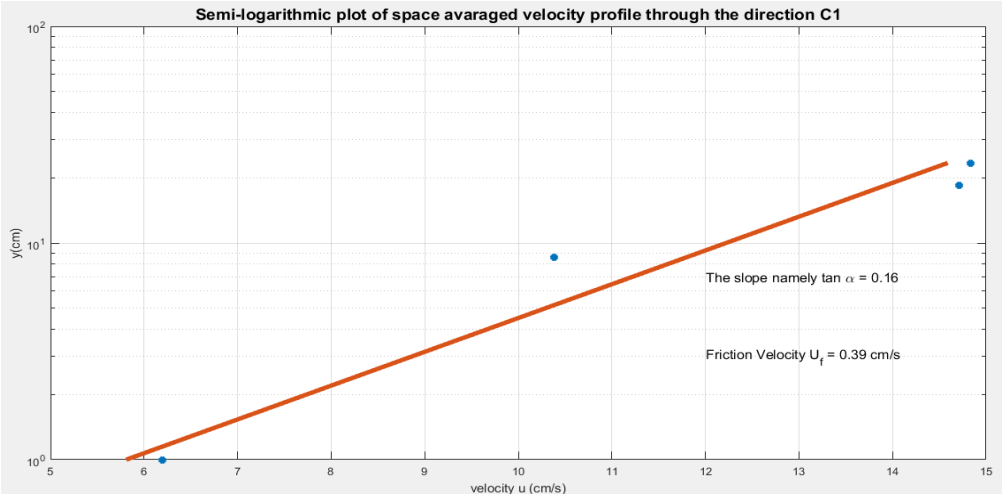

Figure 4.14 : The semi-logarithmic plot of the mean velocity profile through the direction C1.

As the slope of the mean velocity profile is found as 0.16:

$$U_f = \frac{\tan \partial}{\kappa} = \frac{0,16}{0,41} = 0,39 \text{ cm/s} \tag{4.19}$$

$-\rho\overline{U_r'w'}$ is found more purposeful to go on with as it is the resultant magnitude of the both horizontal velocity vectors. Dividing it with the squared friction velocity times the specific weight ρ, $\rho U_f^{\,2}$, the non-dimensional Reynolds stress are obtained:

$$U_f = \sqrt{\frac{\tau_0}{\rho}} \tag{4.20}$$

$$\tau_0 = U_f^{\,2}\ \rho \tag{4.21}$$

$$\tau_{non-\dim ensional} = \frac{-\rho\overline{U_r'w'}}{\rho U_f^{\,2}} \tag{4.22}$$

If the specific weight terms can be abbreviated as the dividend value is going to be positive due to the fact that the fluctuation component $\overline{U_r'w'}$ is negative. The formula can be written as

$$\tau_{non-\dim ensional} = \frac{\overline{U_r'w'}}{U_f^{\,2}} \tag{4.23}$$

At five measurement levels, on five different horizontal planes dimensionless shear stress values are plotted within the scope of the evaluation of the Reynolds stresses in the reservoir. The following figures demonstrate the stresses in contours format. The shear stresses and the dam embankment/the sediment sluicegates/reservoir area are drawn together in order to provide insight on the distribution and the magnitudes of the non-dimensional stresses.

Furthermore, the non-dimensional shear stresses obtained by the following fluctuating components, $\overline{u'w'}$ and $\overline{v'w'}$ are also plotted at five measurement levels. The first five following figures show the non-dimensional shear stresses obtained by $\overline{U_r'w'}$. The second quintet are the ones obtained by $\overline{u'w'}$ components and finally the last quintet demonstrate the shear stresses obtained by $\overline{v'w'}$ components.

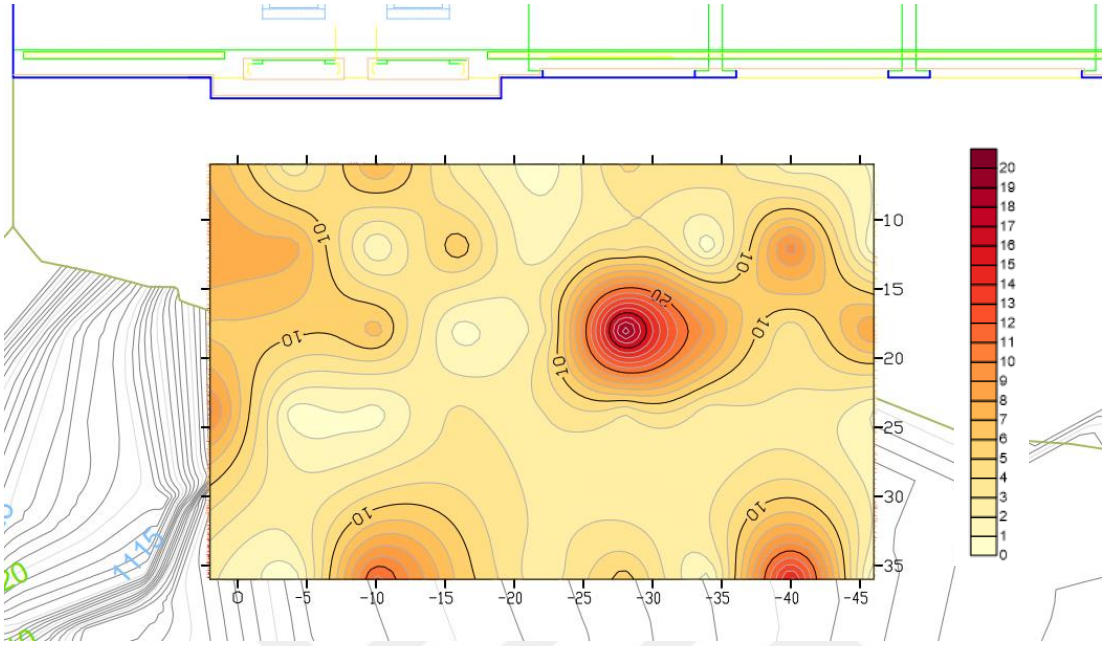

Figure 4.15 : The non-dimensional Reynolds stresses at Z=1108 m.

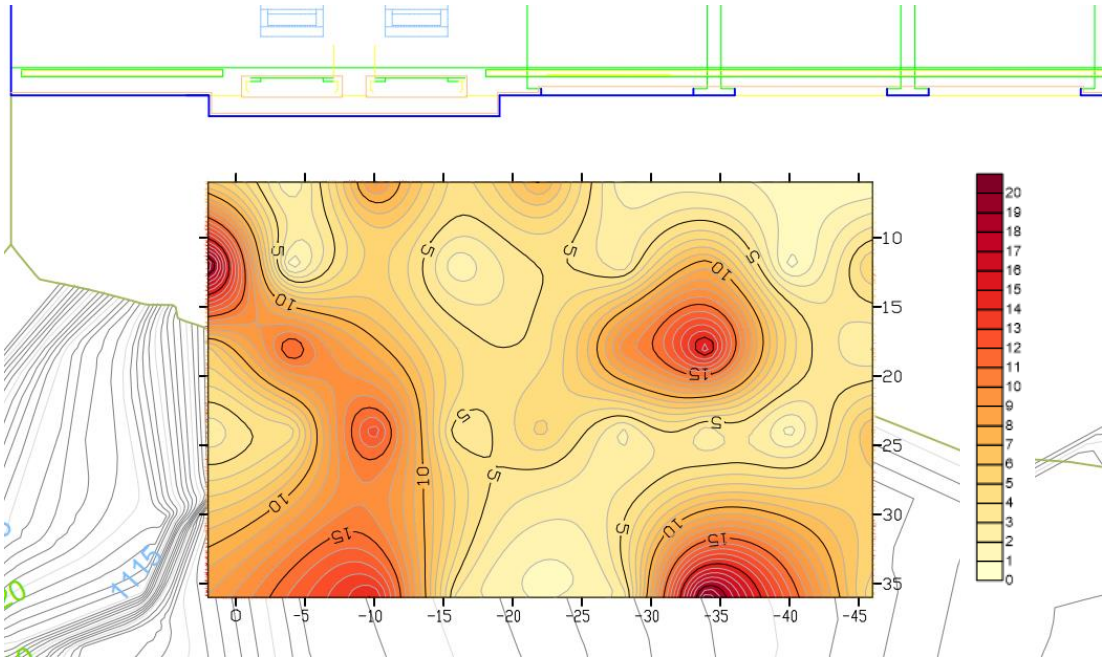

Figure 4.16 : The non-dimensional Reynolds stresses at Z=1110 m.

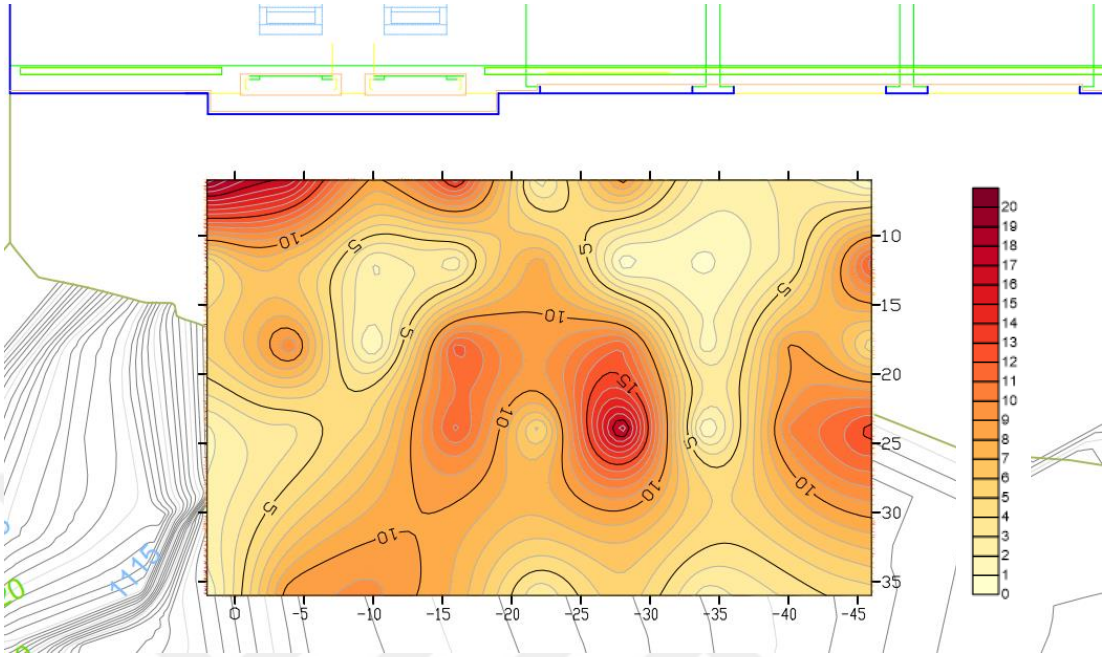

Figure 4.17 : The non-dimensional Reynolds stresses at Z=1111 m.

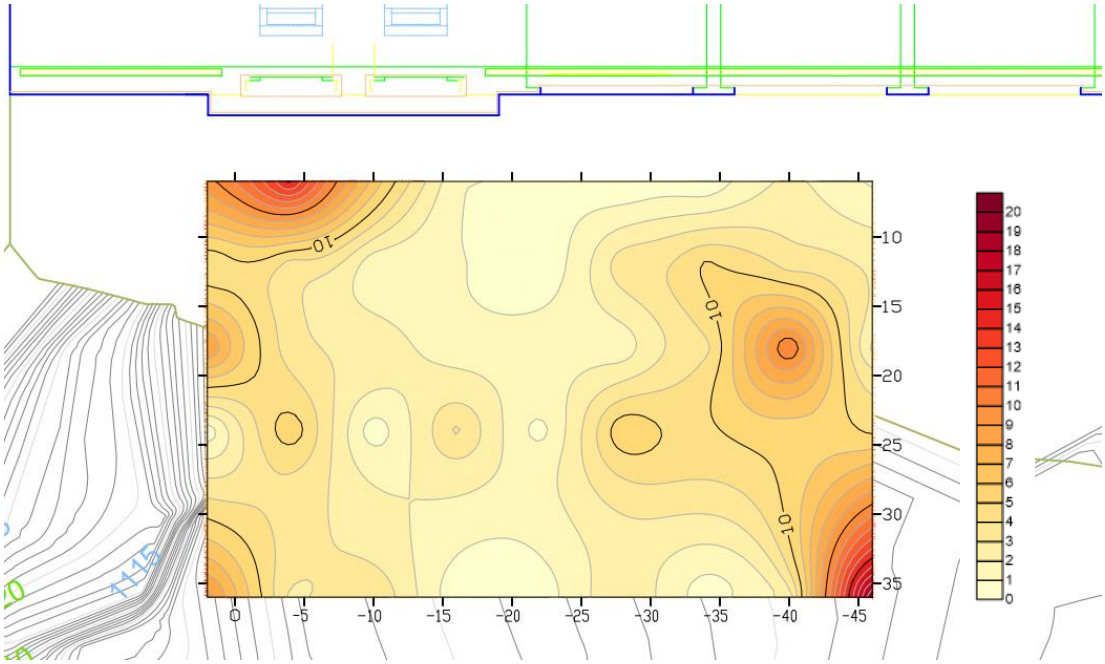

Figure 4.18 : The non-dimensional Reynolds stresses at Z=1113 m.

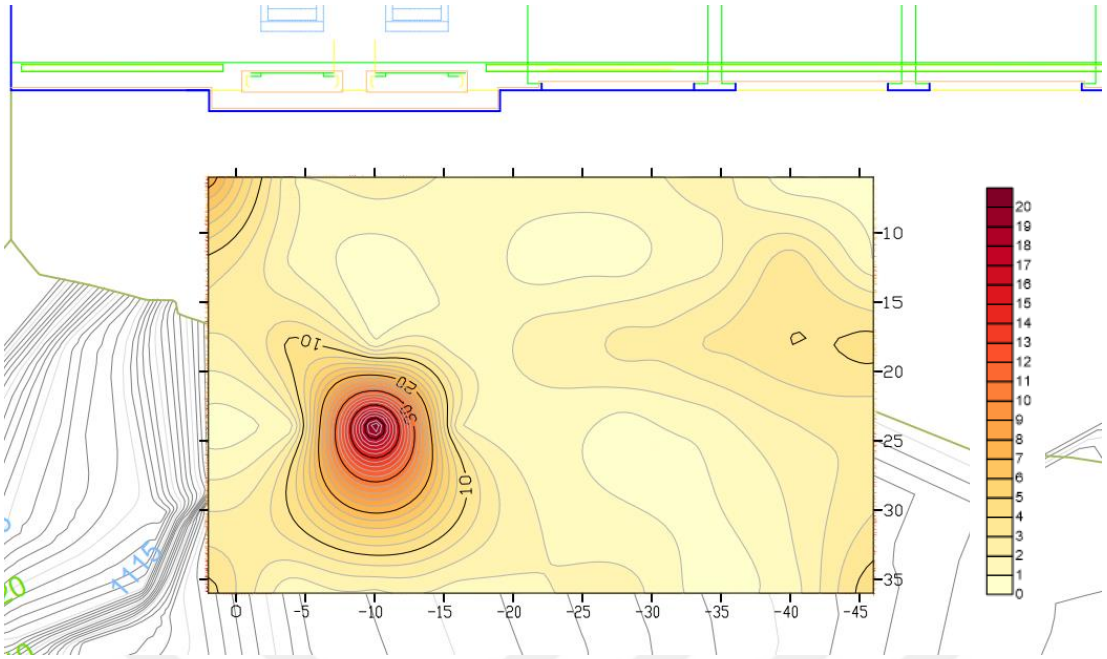

Figure 4.19 : The non-dimensional Reynolds stresses at Z=1118 m.

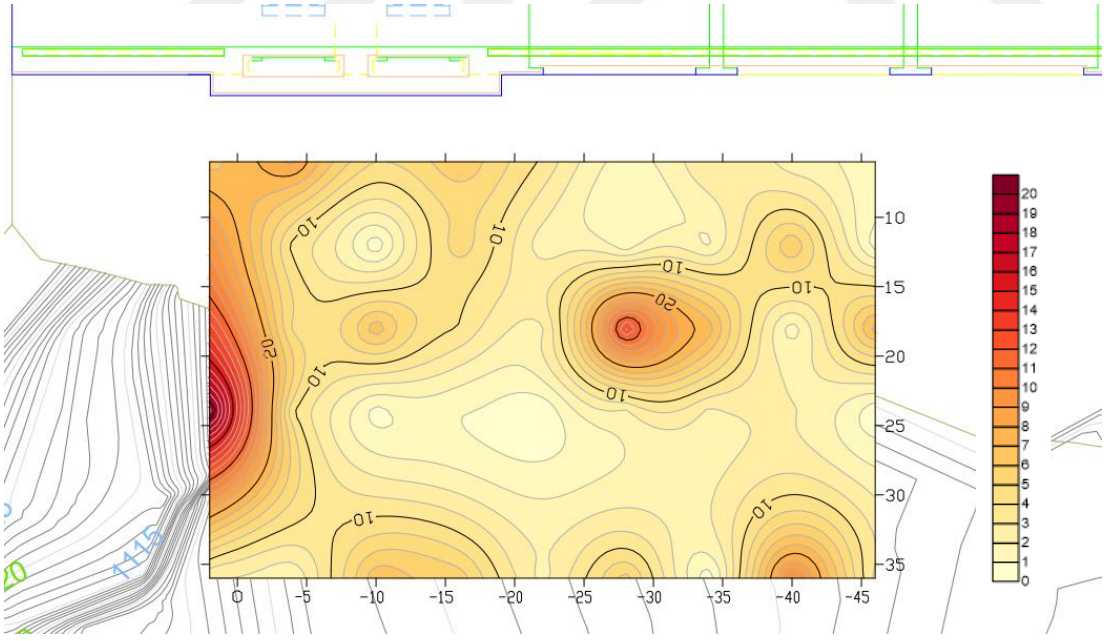

Figure 4.20 : The non-dimensional Reynolds stresses at Z=1108 m ($\frac{\overline{u'w'}}{U_f^2}$).

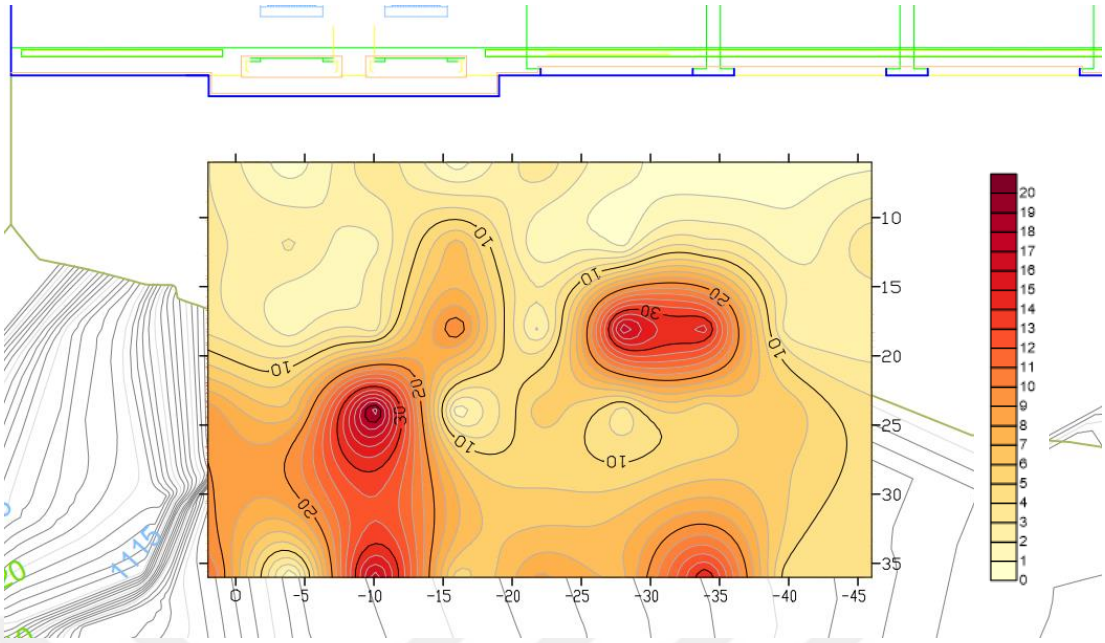

Figure 4.21 : The non-dimensional Reynolds stresses at Z=1110 m ($\frac{\overline{u'w'}}{U_f^2}$).

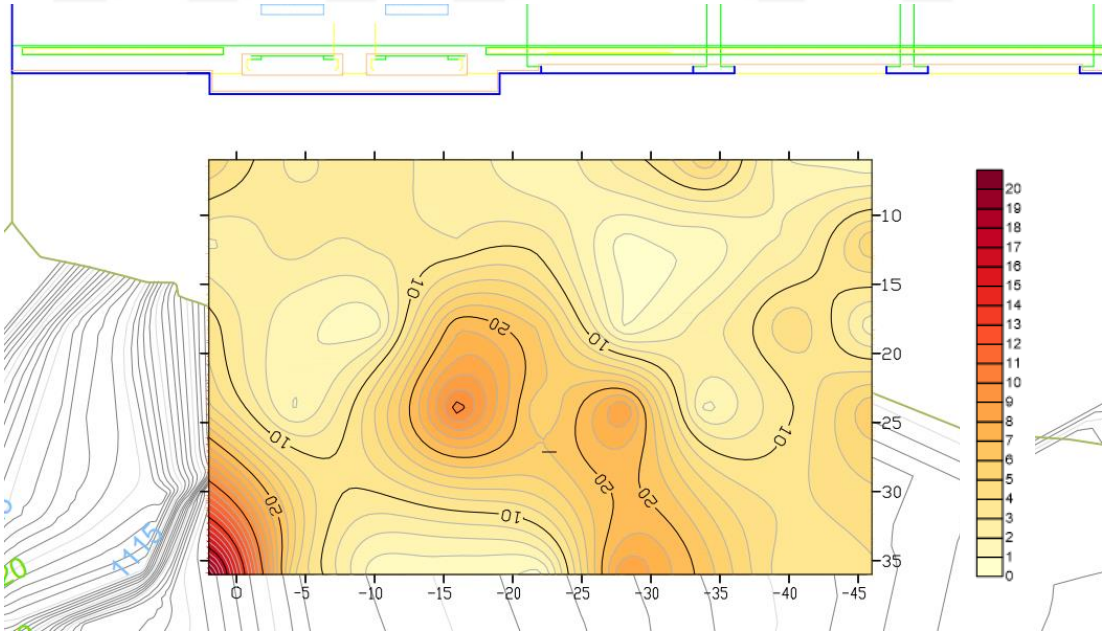

Figure 4.22 : The non-dimensional Reynolds stresses at Z=1111 m ($\frac{\overline{u'w'}}{U_f^2}$).

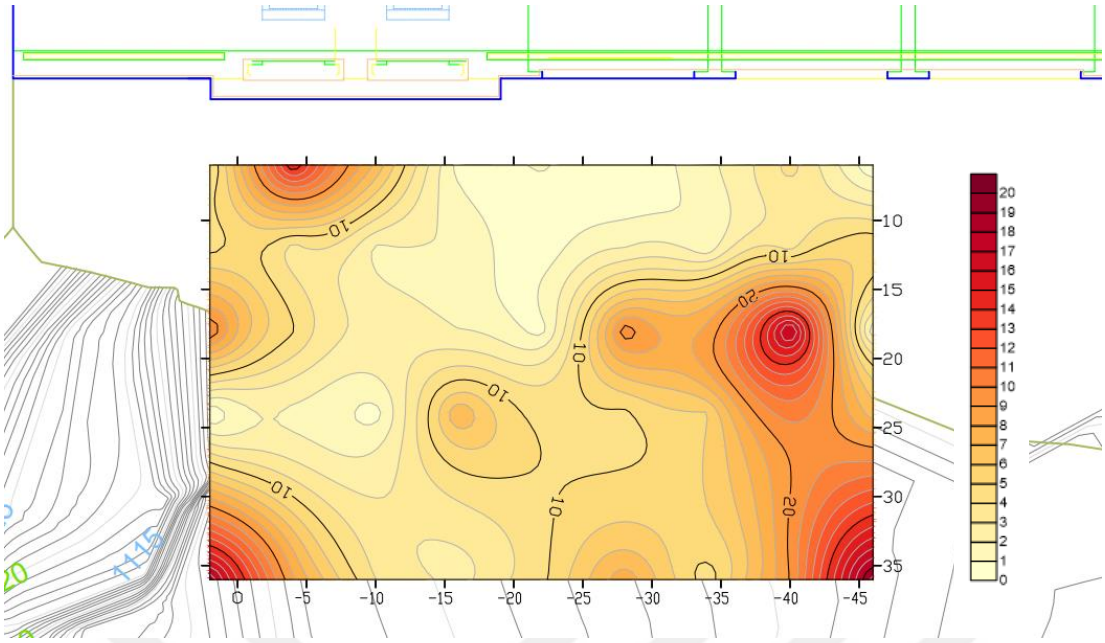

Figure 4.23 : The non-dimensional Reynolds stresses at Z=1113 m ($\frac{\overline{u'w'}}{U_f^2}$).

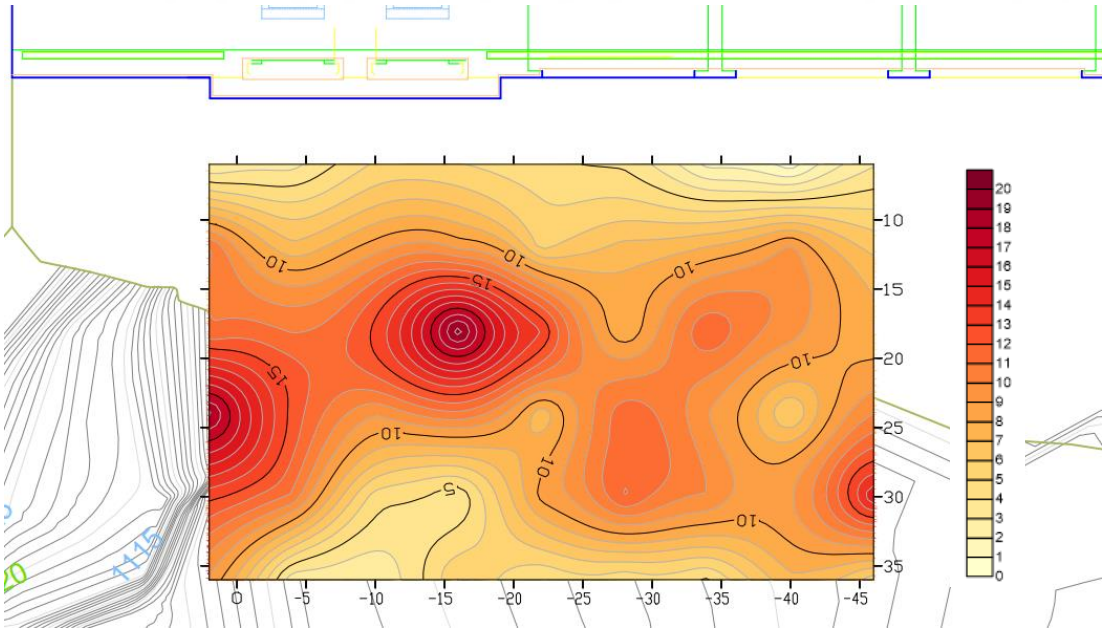

Figure 4.24 : The non-dimensional Reynolds stresses at Z=1118 m ($\frac{\overline{u'w'}}{U_f^2}$).

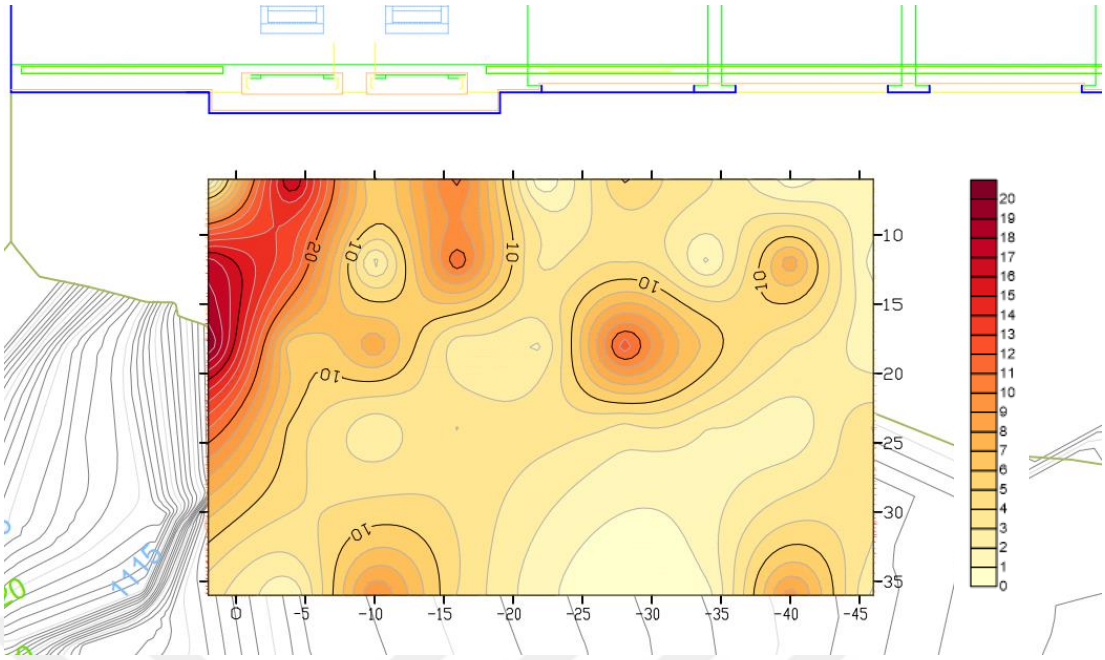

Figure 4.25 : The non-dimensional Reynolds stresses at Z=1108 m ($\frac{\overline{v'w'}}{U_f^2}$).

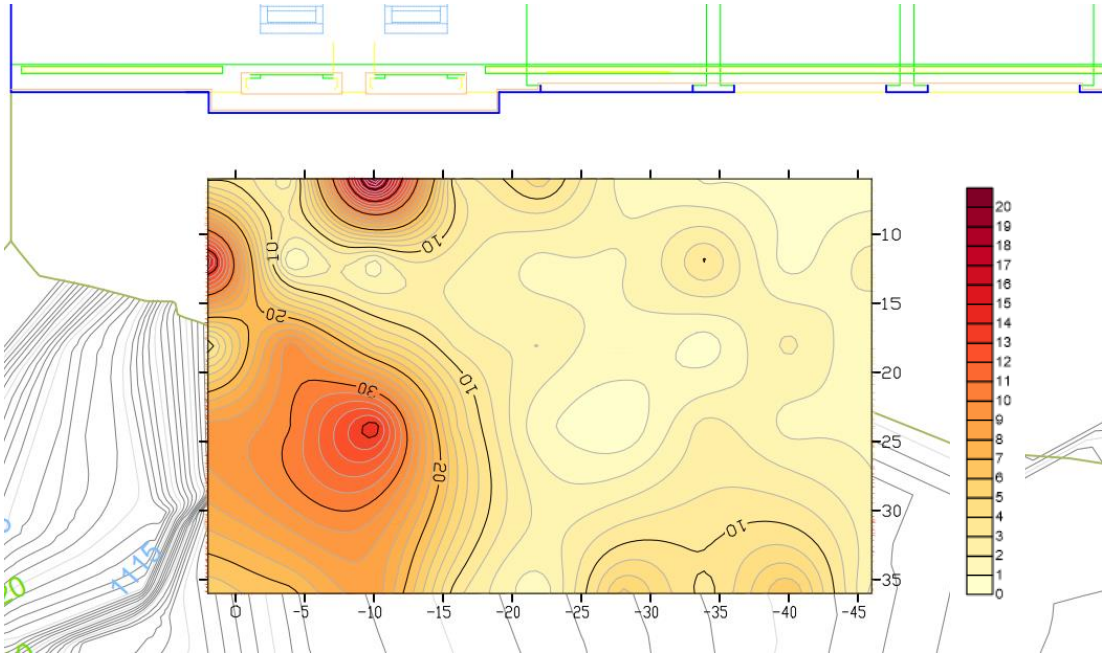

Figure 4.26 : The non-dimensional Reynolds stresses at Z=1110 m ($\frac{\overline{v'w'}}{U_f^2}$).

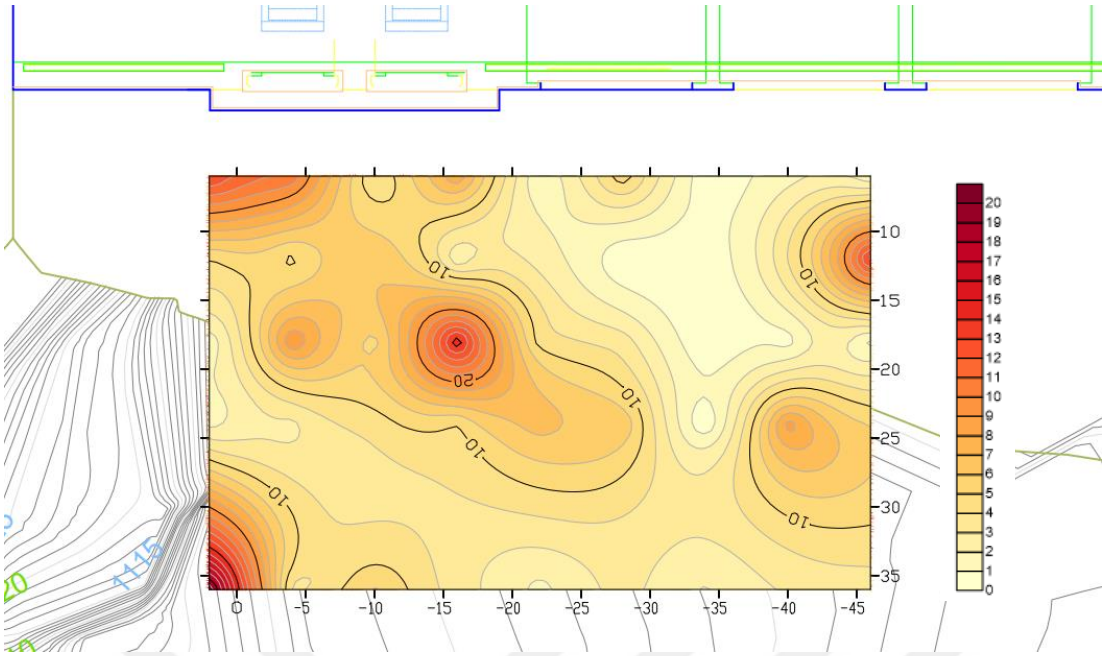

Figure 4.27 : The non-dimensional Reynolds stresses at Z=1111 m ($\frac{\overline{v'w'}}{U_f^{\,2}}$).

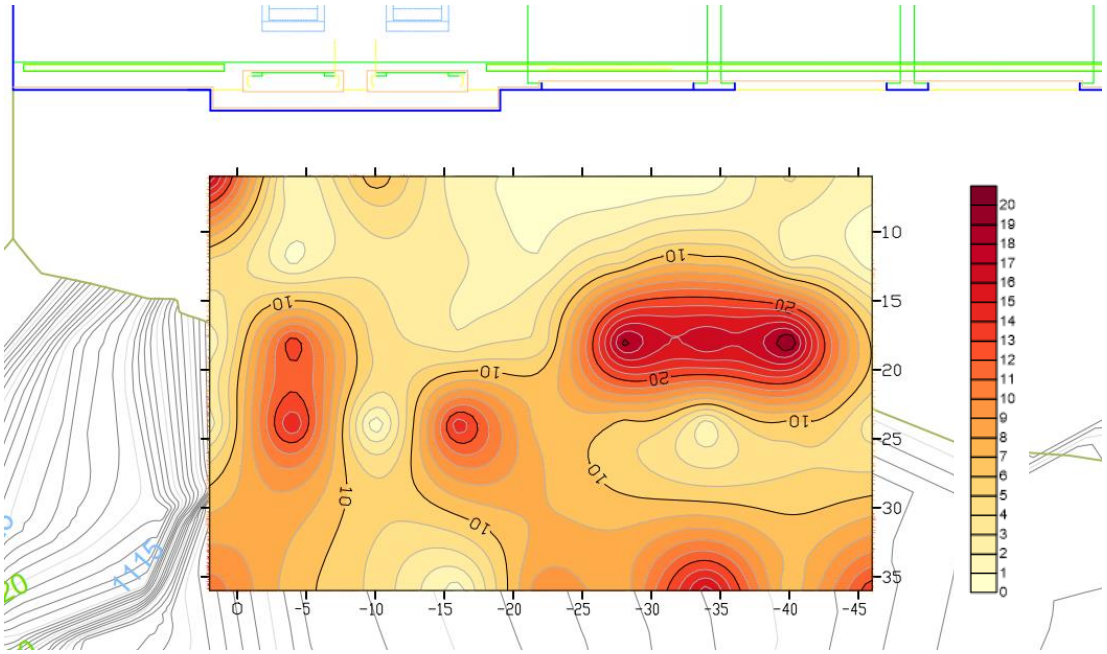

Figure 4.28 : The non-dimensional Reynolds stresses at Z=1113 m ($\frac{\overline{v'w'}}{U_f^{\,2}}$).

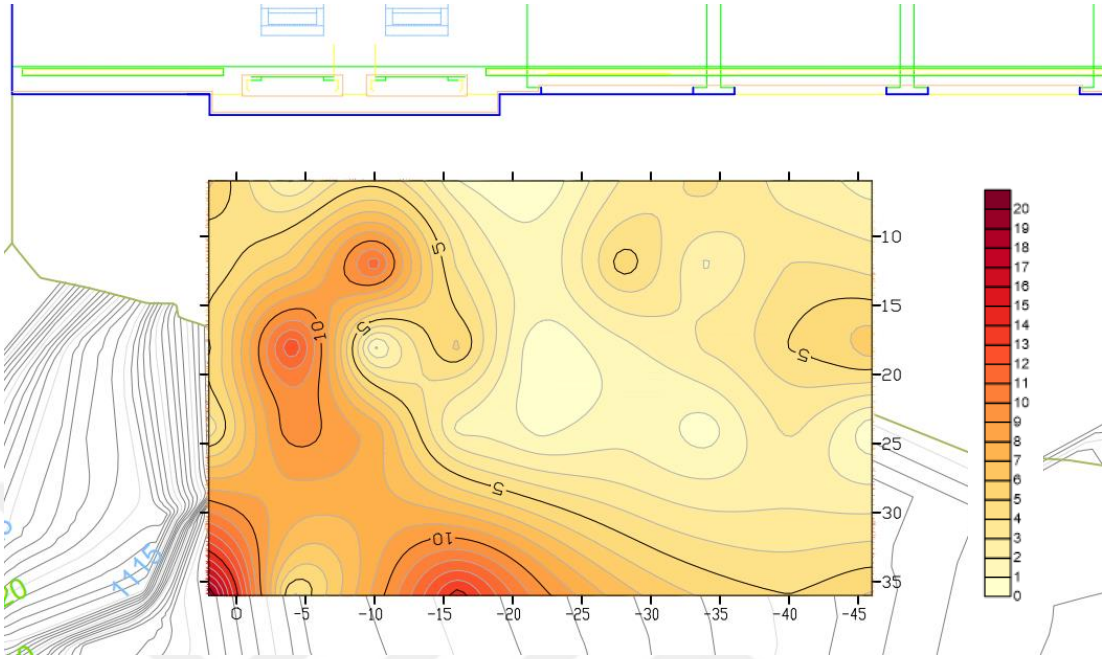

Figure 4.29 : The non-dimensional Reynolds stresses at Z=1118 m ($\frac{\overline{v'w'}}{U_f^2}$).

The contour maps, especially the one at the level of the mid-axis of the sediment sluicegate, Z=1111 m display that the peaks in the meaning of stress develop near the dam embankment and the stresses increase also towards to the left due to the topography of the slope at the left as it is very steep. Furthermore, a tongue shaped trace is observed at the right-hand side on the contour shear stress map of the level 1111 m. Compared to the shape observed in the same area during the experiment, it must be remarked that the two shapes are very similar to each other. The shape observed when the valves were opened can be seen in the Figure 4.30.

Figure 4.30 : The tongue shaped trace observed during the experiments.

In conclusion, because of the topography, in other words having a more complicated geometry than a basic open channel geometry, the stress peaks tend to occur at very different regions as various values. It should be also indicated that as getting to the lower levels, the peaks are seen at unexpected regions due to the vortex developments as the flow moves up to the gates at a certain level/the sediment sluicegate mid-axis level; thus, the contours of the levels, Z=1108 m and Z=1110 m are examples for this circumstance.

4.5 Discussions on the Subject

4.5.1 On scour cone length and volume

As the equilibrium scour cone volume V and length L are basic variables and may respectively expressed as follows according to Moghadam, Emamgholizadeh, Bina and Ghomeshi (2010):

$$\frac{V}{D^3} = f\left(\frac{u}{\sqrt{g(G_S - 1)\,d_{50}}}, \frac{H_w}{H_s}, \frac{\rho_w u D}{\mu}\right)$$
$$\frac{L}{D} = f\left(\frac{u}{\sqrt{g(G_S - 1)\,d_{50}}}, \frac{H_w}{H_s}, \frac{\rho_w u D}{\mu}\right) \quad (4.24)$$

The parameters needed are obtained by using the data and drawings prepared by the designer of the Güllübağ Dam project. The parameters herewith are given below.

$$Q = 431 m^3/s$$
$$A = 17,5 m^2$$
$$\text{velocity scale} = 5,5$$
$$u = 4,49 m/s$$
$$g = 9,81 m/s^2$$
$$\rho_s = 1,04 g/cm^3$$
$$\rho_w = 1,00 g/cm^3$$
$$G_s = \frac{\rho_s}{\rho_w} = 1,04$$
$$d_{50} = 0,0033 m$$
$$H_w = 1114,5 - 1090 = 24,5 m$$
$$H_s = 1133 - 1114,5 = 18,5 m$$

Utilizing the parameter given, these two following equations and non-dimensional results are found.

$$L^* = 8,19\left(\frac{u}{\sqrt{g(G_S - 1)\,d_{50}}}\right)^{0,1}\left(\frac{H_w}{H_s}\right)^{-0,033} \quad (4.25)$$

$$V^* = 5,28\left(\frac{u}{\sqrt{g(G_S - 1)\,d_{50}}}\right)^{0,1}\left(\frac{H_w}{H_s}\right)^{-0,046} \quad (4.26)$$

$$L^* = 8,19\left(\frac{4,49}{\sqrt{9,81(1,04 - 1)0,0033}}\right)^{0,1}\left(\frac{24,5}{18,5}\right)^{-0,033}$$
$$V^* = 5,28\left(\frac{4,49}{\sqrt{9,81(1,04 - 1)0,0033}}\right)^{0,1}\left(\frac{24,5}{18,5}\right)^{-0,046}$$
$$L^* = 13,15$$
$$V^* = 8,45$$

Comparing these two non-dimensional results with the length and volume values measured in the laboratory displays whether the non-dimensional length and volume equilibriums suggested by M. Fathi-Moghadam et al. (2010) are also valid for an open channel problem with complex geometry, not only for a basic open channel problem like theirs.

By multiplying the two results by D and V^3, the dimensional length and volume values, in m and m^3 respectively are found as these magnitudes are needed dimensionally in order to be able to make a comparison between these calculated volume and length values and the measured values during the sluicegate experiments. The dimensional length and volume are calculated as

$$L = L^* D = 13.15 \times 2.92 = 38.4m \tag{4.27}$$

$$V = V^* D^3 = 8.45 \times 2.92^3 = 210.4m^3 \tag{4.28}$$

The results display that the application of the suggested formulas to determine scour cone length and volume is considerably appropriate since the measured length and volume values are 40m and $220m^3$ and the calculated and the measured data are clearly close to each other. The relative error is 4% for both length and volume analysis. It should be also stated that the topography of the Güllübağ Dam's reservoir and therefore the geometry formed in the model is surely more complex than the geometry of a basic open channel for which the scientists in 2010 have suggested the scour cone length and volume formulas. The relative error in percentage is obtained through the following formula, taking y as any variable, in this case L and V:

$$\varepsilon_r = 100 \times \frac{\left| y_{measured} - y_{calculated} \right|}{\left| y_{measured} \right|} \tag{4.29}$$

4.5.2 Evaluation of sediment motion in the reservoir

The Shields' parameter, also called Shields' number or Shields' criterion is a non-dimensional number utilized to calculate the initial motion of the sediment in a fluid flow. As making the shear stress values non-dimensional in this study, Shields' criterion is a nondimensionalization method as well and generally τ^* and θ denote Shields' parameter.

Shields' parameter provides to determine the regions where the sediment accumulation would likely occur as it is a function of shear stress, as shown below the paragraph. This parameter basically provides a connection between grain size and shear stress and can be used for any grid point given within this study. As the coordinates and elevations, namely the grid system has been shown and the shear stress contours are drawn, it is possible to determine any probable sediment accumulation for any point in the grid system. Shields' criterion is expressed as follows:

$$\theta = \frac{\tau}{(\rho_S - \rho)\,\mathrm{gD}} \tag{4.30}$$

Where:

τ is the shear stress;

ρ_s dis the density of the sediment;

ρ_w is the density of the fluid;

g is acceleration due to gravity;

D is a characteristic particle diameter of the sediment.

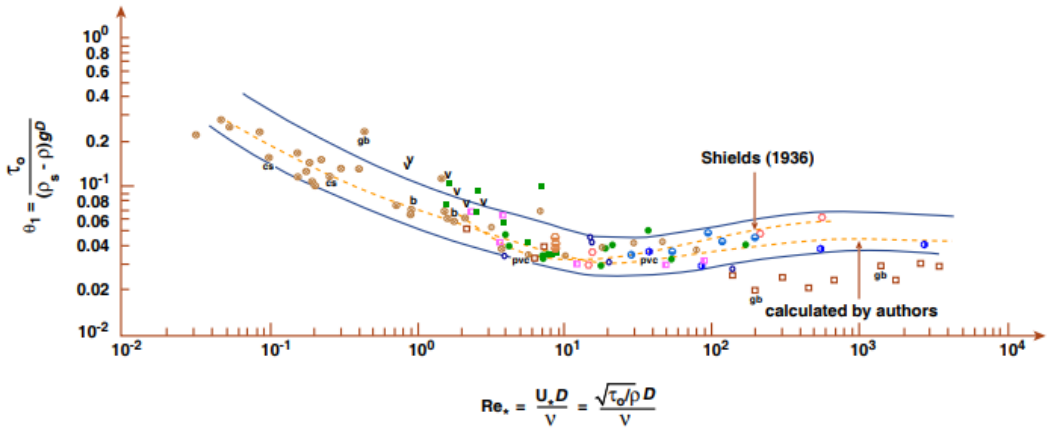

Figure 4.31 : A modified and updated version of the Shields diagram. (From Miller et al., 1977).

The Shields' criterion is applied to each point in the grid system through a basic "for loop" in Matlab to have a maximum value of grain diameter; so that, it is possible to obtain the maximum size of the sediment that can be moved by the flow. In consequence of this calculation, it is revealed that the shear stress of 0.66 Pa (N/m^2) at the point C46 is the highest stress value and therefore allows the initial motion of the

largest sediment particle, which equals to 0.028 m. Under the title 4.4, where Nikuradse's equivalent was presented, D, sediment size was also found as 0.024 m, which is a very close length to 0.028 m. Hence, it could be naturally expressed that the sediments with diameter of 0.028 m or smaller are moveable and thereby flushable in the reservoir. In addition to this, the average diameter of the sediment that starts the initial motion is determined as 0.004 m.

5. CONCLUSION AND RECOMMENDATIONS

The mean velocity profiles, Reynolds stresses and turbulence intensities during the flushing process have been investigated within the scope of this study. The results and the recommendations to create a basis for further works are as follows:

In this study, local flushing takes place, drawdown flushing does not occur and as a result no flushing channel formations are observed. No erosions (retrogressive erosion) occurred in the zones closer to the reservoir inlet.

Even though the flushing cone and scouring volumes are in line with the previous studies, the forms of these volumes show differences. (Shen, 1996; Moghadam, 2010) The most important reasons behind this include:

1) Since our sluice was located not under the sediment volume, but at a slightly higher part of it, the scouring of the sediment brought about the appearance of a trapezoid prism rather than a fully conic appearance.
2) Our sluice is located on the left of the sediment volume and not in the middle of it, therefore, a scouring on the left bank down to the bottom and an oblique scouring on the right bank occurred.

Also, due to these reasons, the talveg line shifted to the left bank due to the effect of the dam structure and more precisely, the position of the sediment sluice.

Again, in line with the previous studies, the flushing sediment volume decreased as the water level increased. When the sediment washout tests are performed with the dam water level kept at 1147 m (max. operation level), spillway channels, tunnel gates and sediment sluice gates wide open), the amount of washed out sediment was found to be 0.046 m^3 in line with the previous experimental studies and a volume of 0.049 m^3 was washed out in the sediment experiments performed with all sediment covers wide open and the water level kept at 1133 m (spillway channel crest).

While a rapid sediment movement and washout took place on the bottom of the sediment sluice inlet and its vicinity, these values gradually declined on the way to the upstream and no movements took place in the reservoir bottom after nearly 30 m for

the polystyrene material (quartz sand with a diameter of 2.5 mm in nature) used in the experiment. It is identified that the washout impact area of the sediment sluice extended to the first spillway inlet section axis towards the right bank. This result indicates that a washout procedure to be performed with the aid of sediment sluice makes it possible to keep a wide enough area clean in front of the tunnel inlet section and to prevent the entrance of any potentially harmful solid particles into the tunnel.

By default, the washout impact area and its dimensions explained above and seen in the figure would be higher if the diameter of sediment deposited in the bottom is smaller than 2.5 mm, the natural corresponding value of the sediment used in the model, and it would be lower if the sediment diameter is larger than 2.5 mm.

It should be kept in mind that it would be possible to wash and remove the deposited thin materials, which accumulated over time in a limited zone in front of the water inlet port by means of such and similar bottom sluices and sediment sluices with enhanced capacity that recently came to be launched in dams and are not consolidated under pressure in time, and that it cannot be expected under any circumstances that the active volume can be maintained by removing all the materials.

It should be also underlined that it is not realistic to expect to use the whole reservoir in full capacity constantly; nevertheless, the non-consolidated sediment accumulations that consist of fine material and form near the water intake can be flushed through the bottom and sluice gates, which have been designed and applied in reservoir projects commonly in recent years.

REFERENCES

Hinze, J.O. (1975): Turbulence. McGraw-Hill.

Bayazıt, M. (1976) Free surface flow in a channel of large relative roughness. *J. Hyd. Research*, 14, No. 2 (1976), p. 115.

Miller, M.C., McCave, I.N., Komar, P.D. (1977) Threshold of sediment motion under unidirectional currents. *Sedimentology 24,* p.507–527

Orszag, S.A., Patera, A.T. (1981). Calculation of Von Karman's constant for turbulent channel flow. *Physical Society Letters*. Vol. 47. No. 12, December.

Grass, A.J. (1983). The influence of boundary layer turbulence on the mechanics. *EUROMECH 156: Mechanics of sediment transport* ed. Sumer & Muller.

Sümer, B. M., Ünsal, I., Bayazıt M. (1983). Hydraulics lecture book in Turkish.

Nezu, I. and Nakagawa, H. (1993): Turbulence in Open-Channel Flow. IAHR Monograph, A.A. Balkema (Roterdam).

Shen, H.W., Lai J.S. (1996). Sustain reservoir useful life by flushing sediment. *International Journal of Sediment Research*. IRTCES, Vol. 11. No. 3, December.

Shen, H.W. (1999). Flushing sediment through reservoirs. *Journal of Hydraulic Research*. Vol. 37. No.6.

Sümer, B. M., Çokgör Ş., and Fredsφe, J. (2001). Suction removal of sediment from between armor blocks. *Journal of Hydraulic Engineering, 127*(4), 293-306

Emamgholizadeh, S., Fathi-Moghadam, M., Bina, M., Ghomeshi, M. (2006). Investigation and evaluation of sediment flushing through storage reservoir. *Journal of Engineering and Applied Sciences*. Vol. 1. No.4, December.

Sedimentation Comittee. (2009). Sedimentation and sustainable use of reservoirs and river systems. *The ICOLD Bulletin,* March 2009.

Fathi-Moghadam, M., Emamgholizadeh, S.,Bina, M., Ghomeshi, M. (2010) Physical modeling of pressure flushing for desilting of non-cohesive sediment. *Journal of Hydraulic Research,* Vol. 48, No. 4 (2010), pp. 509 –514

Avcı, İ., Çokgör Ş., Durmuş, Ö. (2009) Güllübağ Barajı Dolu Savak ve Sediment Savağı Deneyleri. *ITU Hydraulics Laboratory Report prepared in accordance with the request of the contractor firm Soyak Enerji*

CURRICULUM VITAE

Name Surname	**:** Erdem ÇELENK
Place and Date of Birth	**:** Bursa / 20.02.1993
E-Mail	**:** celenke@itu.edu.tr

EDUCATION:

- **B.Sc.:** 2017, Istanbul Technical University, Civil Engineering Faculty, Civil Engineering Department
- **M.Sc.:** 2020, Istanbul Technical University, Civil Engineering Faculty, Hydraulics and Water Resources Engineering Program

PROFESSIONAL EXPERIENCE:

- **2017-2018:** Design Engineer, 4D Engineering
- **2018-Present:** Design Engineer, Prota Engineering